Development of highly immunogenic vaccine by using dendritic cell-targeting bio-nanocapsule

名古屋大学大学院生命農学研究科

生命技術科学専攻

生物機能技術科学講座

産業生命工学研究分野

松尾　英典

2014 年 3 月

Contents

Chapter IV

Comprehensive discussion

Abbreviations

Ag	antigen
APC	Ag-presenting cell
BNC	bio-nanocapsule
BS^3	bis-sulfosuccinimidyl suberate
CLR	C-type lectin receptor
COV	cut-off value
CR4	complement receptor 4
CTL	cytotoxic T lymphocyte
DC	dendritic cell
DDS	drug delivery system
DLS	dynamic light scattering
EGFR	epidermal growth factor receptor
ELISA	enzyme-linked immunosorbent assay
fOVA	fluorophore (CF488A)-labeled ovalbumin
HBV	hepatitis B virus
HRP	horseradish peroxidase
IM	intramuscular
IV	intravenous
JEV	Japanese encephalitis virus
LD_{50}	50% lethal dose
LN	lymph node
LP	liposome
LPS	lipopolysaccharide

LSM	laser scanning microscopy
MHC	major histocompatibility complex
OVA	ovalbumin
PBS	phosphate buffered saline
PRR	pattern recognition receptor
QCM	quartz crystal microbalance
SC	subcutaneous
SPDP	N-succinimidyl- 3-(2-pyridyldithio) propionate
SPF	specific pathogen-free
sulfo-LC-SPDP	sulfosuccinimidyl 6-[3´(2-pyridyldithio)-propionamido] hexanoate
Th cell	helper T cell
TMB	3,3’-5,5’-tetramethylbenzidine

Chapter I

General introduction

1.1. General introduction

Vaccination has been accepted as a successful medical mean to prevent various infectious diseases in the world. As the first 'vaccine', Dr. Edward Jenner demonstrated at the end of 18th century that cowpox-infected materials could be effective for immunization against smallpox virus. In 20th century, virus attenuating techniques have been developed for live attenuated vaccines against measles, mumps, and rubella [1-4]. By the latter part of the 20th century, most of the vaccines that could be developed by direct mimicry of natural infection with live attenuated or killed/inactivated vaccines (*e.g.*, polio vaccine, influenza vaccine, rabies vaccine). Although these vaccines have significantly contributed to the prevention of infectious diseases, a part of vaccines are still less effective for providing vaccinees with sufficient protective immunities (*e.g.*, HIV vaccine, malaria vaccine). Moreover, some conventional vaccines contain pathogen-derived components, which inflict adverse side effects unexpectedly. For overcoming these drawbacks of conventional vaccines, since pathogen-derived components of neither infectivity nor toxicity were expected as ideal antigens (Ags), they have been produced by recombinant DNA technology. However, the vaccines formulated with these components (*i.e.*, subunit vaccines) have been revealed less immunogenic than conventional vaccines consisting of whole viruses. Low complexity of component surface might reduce the recognition by Ag-presenting cells (APCs) through pattern recognition receptors (PRRs including Toll-like receptors), leading to the low immunogenicity of subunit vaccines [5]. For

enhancing the immunogenicity of subunit vaccines, drug delivery system (DDS) has been considered as a promising platform for delivering vaccine Ags to APCs [6, 7]. Especially, dendritic cells (DCs), a major member of APCs, stimulate naïve T cells more effectively than other APCs such as macrophages and B cells [8-11]. Thus, DCs have been considered as most promising target cells for Ag delivery to elicit effective immunity against exogenous pathogens. Generally, DDS-based vaccines are classified into instruments and nanocarriers. The former utilizes microneedles and injectors for administrating Ags to specific sites of the body, facilitating the delivery of Ags specifically to Langerhans cells and migratory DCs, respectively [12, 13]. The latter utilizes the particle structure of nanocarriers for efficient recognition and incorporation of Ags by DCs in a passive manner [14].

Although some DDS-based vaccines achieved the DC-specific Ag-delivery, these vaccines could not induce the sufficient level of immune responses without adjuvants. It has been considered necessary for inducing effective adaptive immunities to elicit innate immunity with conventional adjuvants (*e.g.*, Alum, Freund's adjuvants, and ligands of Toll-like receptors) [15]. Some components of these adjuvants interact with PRRs and thereby stimulate the maturation of DCs for effective Ag-presenting to naïve T cells. However, either non-specific or over elicitation of innate immunity by adjuvants should be avoided for the guarantee of their safety, because host cells generally express PRRs. In addition, it remains unsettled how a part of adjuvants could elicit innate immunity on the molecular basis. These situations have led me to consider that adjuvants should work on DCs specifically and mount adjuvant activity on DC-targeting nanocarriers [16].

Bio-nanocapsule (BNC), an approximately 50-nm hollow nanoparticle consisting of hepatitis B virus (HBV) surface Ag L protein, can be synthesized in

recombinant *Saccharomyces cerevisiae* efficiently (up to 40 % (w/w) of soluble total protein) [17]. According to the HBV-derived early infection machinery, BNC could deliver payloads (DNA, chemical compounds) to human hepatocyte specifically. Initially, BNC could encapsulate payloads into the hollow space by electroporation (1st generation encapsulation method). While the complex could deliver payloads to human hepatocytes specifically and efficiently [18, 19], the electroporation method was not applicable to the mass production of BNC-based medicines. Next, BNC was found to possess membrane fusogenic activity, facilitating spontaneous complex formation of payload-encapsulated liposomes (LPs) and BNCs (2nd generation encapsulation method) [20]. The BNC-LP complexes could deliver payloads specifically to human hepatocytes with comparable level of transfection efficiency. Furthermore, it is expected that the membrane fusogenic activity of BNC contributes to the endosomal escape of payloads. Recently, our group have modified BNCs (ZZ-BNCs) without affecting on the membrane fusogenic activity, which display tandem form of *Staphylococcus aureus* protein A-derived IgG Fc-binding Z domain [21, 22]. The ZZ-BNCs allowed us to integrate IgG of interest and exhibit the Fv regions of IgGs outwardly for effective binding of Ags in an oriented-immobilization manner [23]. ZZ-BNCs displaying IgGs against EGFR (epidermal growth factor receptor) could target EGFR-overexpressing glioblastoma efficiently *in vivo* through intracerebroventricular injection [22]. Thus, these situations have led me to evaluate the potential of BNC technology in DC-specific Ag delivery.

Firstly, for re-targeting ZZ-BNC to DCs, I have investigated DC-specific surface Ags. In Chapter II, as various DC-specific receptors (*e.g.*, integrin, C-type lectin, Fc receptor) had been utilized for the DC-targeting of nanocarriers [24], the IgGs against these receptors were integrated onto ZZ-BNCs, and then the α-DC

IgG-ZZ-BNC complexes were examined for the *in vitro* attachment and *in vivo* accumulation to splenic DCs. Finally, α-CD11c IgGs was found to confer sufficient *in vivo* DC-targeting ability on ZZ-BNC, and therefore the complex of ZZ-BNC and α-CD11c IgG (hereafter referred as α-DC-ZZ-BNC) was used for further experiments. When α-DC-ZZ-BNC was fused with Ag-loaded cationic LPs and then injected systemically to mice, the immunogenicity of the complex was revealed extremely higher than that of Ag itself, suggesting that the α-DC-ZZ-BNC-LP complex is a promising platform for forthcoming vaccines. Meanwhile, the complex could not elicit sufficient immunological responses through local administrations (subcutaneous route, SC; intramuscular route, IM), of which the positive charge might increase non-specific binding *in vivo* and thereby make less being recognized by DCs around injection site. This situation strongly suggested that the complex could not be applied through conventional administration routes (*i.e.*, local administrations), which have been employed at worldwide clinical sites. In Chapter III, for optimizing the particle properties (*e.g.*, size, charge) of α-DC-ZZ-BNC-based vaccines, the Ag-incorporation method was changed from LP fusion to chemical crosslinking. The Ag-crosslinked α-DC-ZZ-BNC (α-DC-ZZ-BNC-Ag) could deliver Ags into DCs efficiently *in vitro*. Through local administration, the α-DC-ZZ-BNC could efficiently accumulate to DCs in lymph nodes (LNs) closest to injection site. The α-DC-ZZ-BNC-Ag could induce efficient DC maturation without any adjuvant, followed by the efficient induction of Ag-specific cellular and humoral immunities. Furthermore, the α-DC-ZZ-BNC complex containing Japanese encephalitis virus (JEV) envelope-derived Ag was found to elicit sufficient protective immunity against the challenge of JEV. Collectively, these results indicated that the DC-specific Ag delivery system utilizing

α-DC-ZZ-BNC is a promising DDS-based vaccine platform for inducing robust immune responses.

1.2. References

1. J.F. Enders, T.H. Weller, F.C. Robbins, Cultivation of the lansing strain of poliomyelitis virus in cultures of various human embryonic tissues, Science 109 (1949) 85-87.
2. S.A. Plotkin, J.D. Farquhar, M. Katz, F. Buser, Attenuation of RA 27-3 rubella virus in WI-38 human diploid cells, Am. J. Dis. Child 118 (1969) 178-185.
3. J.E. Salk, U. Krech, J.S. Youngner, B.L. Bennett, L.J. Lewis, P.L. Bazeley, Formaldehyde treatment and safety testing of experimental poliomyelitis vaccines, Am. J. Public Health Nations Health 44 (1954) 563–70.
4. M.R. Hilleman, E.B. Buynak, R.E. Weibel, J. Stokes Jr, J.E. Whitman Jr, M.B. Leagus, Development and evaluation of the Moraten measles virus vaccine, JAMA 206 (1968) 587-590.
5. D.T. O'Hagan, N.M. Valiante, Recent advances in the discovery and delivery of vaccine adjuvants, Nat. Rev. Drug Discov. 2 (2003) 727–735.
6. J.P. Amorij, G.F.A. Kersten, V. Saluja, W.F. Tonnis, W.L.J. Hinrichs, B. Slütter, S.M. Bal, J.A. Bouwstra, A. Huckriede, W. Jiskoot, Towards tailored vaccine delivery: needs, challenges and perspectives, J. Control. Release 161 (2012) 363–376.
7. Y. Krishnamachari, S.M. Geary, C.D. Lemke, A.K. Salem, Nanoparticle delivery systems in cancer vaccines, Pharm. Res. 28 (2011) 215–236.
8. E.S. Trombetta, I. Mellman, Cell biology of antigen processing *in vitro* and *in vivo*, Annu. Rev. Immunol. 23 (2005) 975–1028.

9. J. Banchereau, F. Briere, C. Caux, J. Davoust, S. Lebecque, Y. Liu, B. Pulendran, K. Palucka, Immunobiogy of dendritic cells, Immunology 18 (2000) 767–811.

10. B.M.L. Albert, S.F.A. Pearce, L.M. Francisco, B. Sauter, P. Roy, R.L. Silverstein, N. Bhardwaj, Immature dendritic cells phagocytose apoptotic cells via $\alpha_v\beta_5$ and CD36, and cross-present antigens to cytotoxic T lymphocytes, J. Exp. Med. 188 (1998) 1359–1368.

11. K. Inaba, R.M. Steinman, Accessory cell-T lymphocyte interactions. Antigen-dependent and -independent clustering, J. Exp. Med. 163 (1986) 247-261.

12. S.P. Sullivan, D.G. Koutsonanos, M. Del Pilar Martin, J.W. Lee, V. Zarnitsyn, S.O. Choi, N. Murthy, R.W. Compans, I. Skountzou, M.R. Prausnitz, Dissolving polymer microneedle patches for influenza vaccination, Nat. Med. 16 (2010) 915–920.

13. J.K. Simon, M. Carter, M.F. Pasetti, M.B. Sztein, K.L. Kotloff, B.G. Weniger, J.D. Campbell, M.M. Levine, Safety, tolerability, and immunogenicity of inactivated trivalent seasonal influenza vaccine administered with a needle-free disposable-syringe jet injector, Vaccine. 29 (2011) 9544–9550.

14. L.J. Cruz, P.J. Tacken, F. Rueda, J.C. Domingo, F. Albericio, C.G. Figdor, Targeting nanoparticles to dendritic cells for immunotherapy, Methods Enzymol 509 (2012) 143-163.

15. A. Iwasaki, R. Medzhitov, Regulation of adaptive immunity by the innate immune system, Science 327 (2010) 291–295.

16. D.M. Smith, J.K. Simon, J.R. Baker, Applications of nanotechnology for immunology, Nat. Rev. Immunol. 13 (2013) 592–605.

17. S. Kuroda, S. Otaka, T. Miyazaki, M. Nakao, Y. Fujisawa, Hepatitis B virus envelope L protein particles. Synthesis and assembly in *Saccharomyces cerevisiae*, purification and characterization, J. Biol. Chem. 267 (1992) 1953–1961.

18. T. Yamada, Y. Iwasaki, H. Tada, H. Iwabuki, M.K.L. Chuah, T. VandenDriessche, H. Fukuda, A. Kondo, M. Ueda, M. Seno, K. Tanizawa, S. Kuroda, Nanoparticles for the delivery of genes and drugs to human hepatocytes, Nat. Biotechnol. 21 (2003) 885–890.

19. Y. Matsuura, H. Yagi, S. Matsuda, O. Itano, K. Aiura, S. Kuroda, M. Ueda, Y. Kitagawa, Human liver-specific nanocarrier in a novel mouse xenograft model bearing noncancerous human liver tissue, Eur. Surg. Res. 46 (2011) 65–72.

20. J. Jung, T. Matsuzaki, K. Tatematsu, T. Okajima, K. Tanizawa, S. Kuroda, Bio-nanocapsule conjugated with liposomes for *in vivo* pinpoint delivery of various materials., J. Control. Release 126 (2008) 255–264.

21. N. Kurata, T. Shishido, M. Muraoka, T. Tanaka, C. Ogino, H. Fukuda, A. Kondo, Specific protein delivery to target cells by antibody-displaying bionanocapsules, J. Biochem. 144 (2008) 701–707.

22. Y. Tsutsui, K. Tomizawa, M. Nagita, H. Michiue, T. Nishiki, I. Ohmori, M. Seno, H. Matsui, Development of bionanocapsules targeting brain tumors, J. Control. Release. 122 (2007) 159–164.

23. M. Iijima, H. Kadoya, S. Hatahira, S. Hiramatsu, G. Jung, A. Martin, J. Quinn, J. Jung, S.Y. Jeong, E.K. Choi, T. Arakawa, F. Hinako, M. Kusunoki, N. Yoshimoto, T. Niimi, K. Tanizawa, S. Kuroda, Nanocapsules incorporating IgG Fc-binding domain derived from *Staphylococcus aureus*

protein A for displaying IgGs on immunosensor chips, Biomaterials 32 (2011) 1455–1464.

24. M.D. Joshi, W.J. Unger, G. Storm, Y. van Kooyk, E. Mastrobattista, Targeting tumor antigens to dendritic cells using particulate carriers, J. Control. Release 161 (2012) 25–37.

Chapter II

Engineered bio-nanocapsules, hepatitis B virus surface antigen L protein particles, for *in vivo* active targeting to splenic dendritic cells

2.1. Abstract

DCs are key regulators of adaptive T-cell responses. By capturing exogenous Ags and presenting Ag-derived peptides via MHC molecules to naïve T cells, DCs induce Ag-specific immune responses *in vivo*. In order to induce effective host immune responses, active delivery of exogenous Ags to DCs is considered important for future vaccine development. Our group recently generated BNCs consisting of HBV surface Ags that mediate stringent *in vivo* cell targeting and efficient endosomal escape, and after the fusion with LPs containing therapeutic materials the BNC-LP complexes that deliver them to human liver-derived tissues *in vivo*. BNCs were further modified to present the IgG Fc-interacting domain (Z domain) derived from *Staphylococcus aureus* protein A in tandem. When mixed with IgGs, modified BNCs (ZZ-BNCs) displayed the IgG Fv regions outwardly for efficient binding to Ags in an oriented-immobilization manner. Due to the affinity of the displayed IgGs, the IgG-ZZ-BNC complexes accumulated at specific cells and tissues *in vitro* and *in vivo*. After mixing ZZ-BNCs with antibodies against DCs, I used immunocytochemistry to examine which antibodies delivered ZZ-BNCs to mouse splenic DCs following intravenous (IV) injection of the ZZ-BNCs. ZZ-BNCs displaying α-CD11c monoclonal antibodies (α-CD11c-ZZ-BNCs) were found to accumulate with about 62% of splenic DCs, and reside within some of them. After the fusion with LPs containing Ags, the α-CD11c-ZZ-BNCs could elicit respective antibodies more

efficiently than other non-targeting control vaccines, suggesting that this DC-specific nanocarrier is promising for forthcoming vaccines.

2.2. Introduction

DCs are a type of APC that are distributed in LNs, spleen, thymus, skin and blood [1, 2]. APCs incorporate exogenous Ags by endocytosis, execute their processing into fragments, and then immediately display them for the recognition by adaptive naïve T cells [2, 3]. Subsequently, the T cells activate humoral and cellular immune responses against the exogenous Ags. In particular, DCs are significantly more effective in T cell stimulation than other APCs such as macrophages and B cells [4, 5], indicating that DCs play a central role in immune defense against exogenous pathogens.

Recently, DC-targeting nanocarriers have been developed for effective vaccine by DC-specific delivery of Ag-encoding genes or exogenous Ags. For example, the replication-defective forms of lymphocytic choriomeningitis virus [6, 7], coronavirus [8], and lentivirus displaying Sindbis virus glycoprotein [9] have been used for DC-specific gene delivery. However, these vectors still present potential problems commonly observed in viral vectors, including unexpected immunological responses in patients, accidental disturbance of patient's chromosomes, and unacceptability for Ags other than DNA. Non-viral vectors have also been utilized for delivering Ags to DCs. Nanoparticles consisting of poly (γ-glutamic acid) could target DCs passively through systemic administration [10]. Micelles consisting of poly (ethylene glycol)-based amphipathic polymer could accumulate in nearly 20% of DCs in draining LNs following intradermal injection [11]. LPs and Ags, modified with Fv forms of α-CD11c [12, 13], bacterial flagellin-related peptide [14], and mannose [15] could target DCs more efficiently than passive targeting due to their specific interactions with DC surface molecules. Although these non-viral vectors may in part solve the viral vector-related problems described above, they potentially lack the

mechanisms for infection and endosomal escape (*e.g.*, membrane fusiogenic domain of viral envelope proteins), leading to reduced immunogenicity of Ags due to low recognition efficiency of DCs. Therefore, it is necessary to endow non-viral vectors with both targeting ability and membrane fusiogenic activity in order to develop effective DC-targeting nanocarriers for future vaccines.

BNCs are approx. 50-nm hollow nanoparticles consisting of about 110 molecules of HBV surface Ag L protein and unilamellar LP [16]. BNCs are produced efficiently in recombinant yeast engineered to express L protein [17, 18]. BNCs specifically attach to human hepatic cells via the N-terminal half of L protein (pre-S1 region), and enter into the cells at the same rate as HBV [19]. Following encapsulation of various materials (genes, proteins, chemical compounds) by electroporation and liposomal fusion, BNCs deliver them specifically to human hepatic cells not only *in vitro* but also *in vivo* [20, 21]. Our group has replaced the central part of the pre-S1 region (amino acid residues 51 to 159) of BNC with a tandem form of the IgG Fc-interacting region (Z domain) derived from *Staphylococcus aureus* protein A [22] to generate ZZ-L protein [23] (Fig. 2.1A). The mutated BNC (ZZ-BNC) can tether IgG Fc regions and display IgG Fv regions outwardly for effective binding of Ags in an oriented-immobilization manner (Fig. 2.1B) [24], while retaining membrane fusiogenic activity. ZZ-BNCs displaying α-EGFR antibodies efficiently targeted EGFR-overexpressing glioblastoma *in vivo* following intracerebroventricular injection [25]. These properties of ZZ-BNCs may be useful for active targeting and introduction of Ags to DCs, making DC-mediated vaccination a promising approach. In this study, ZZ-BNCs displaying α-DC antibodies (α-DC-ZZ-BNCs) were evaluated for both targeting and introduction into splenic DCs *in vitro* and *in vivo*. The α-DC-ZZ-BNCs could be used for DC-specific nanocarriers following the fusion with LPs containing

Ags.

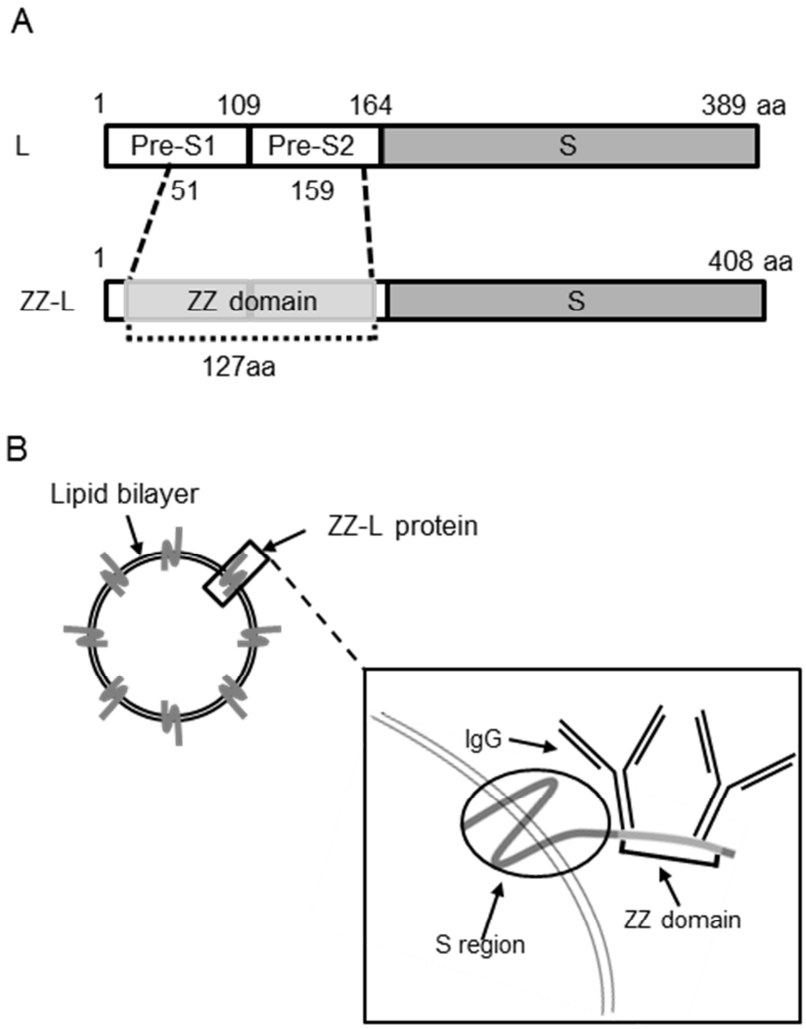

Fig. 2.1 Schematic representation of ZZ-BNCs.
(A) Molecular organizations of HBsAg L protein (upper) and ZZ-L protein (lower). The numbers indicate amino acid residues (aa) at domain borders. (B) Structure of approx. 50-nm diameter ZZ-BNCs. About 120 molecules of ZZ-L protein are embedded in a LP by integration of their S regions into the lipid bilayer. Two IgGs potentially associate with ZZ domain, which is displayed on the surface of ZZ-BNCs.

2.3. Material and methods

2.3.1. Materials

BNCs and ZZ-BNCs were overexpressed in *Saccharomyces cerevisiae* AH22R$^-$ cells carrying the BNC- and ZZ-BNC-expression plasmids, pGLDLIIP39-RcT [17] and pGLD-ZZ50 [23], respectively. BNCs and ZZ-BNCs were purified as described previously [18, 26]. Protein concentrations were determined with a BCA protein assay kit (Pierce, Rockford, IL, USA) using bovine serum albumin (BSA; Wako Pure Chemical Industries, Osaka, Japan) as a control protein. BNC was labeled with a Fluorolink Cy5 mono-functional reactive dye (GE Healthcare) and CF750 NHS ester (Biotium, Heyward, CA, USA) according to the manufacturer's protocol. Z-averages and ζ-potentials of ZZ-BNCs were measured in water at 25°C with a dynamic light scattering (DLS) model Zetasizer Nano ZS (Malvern Instruments, Worcestershire, UK).

2.3.2. Antibodies

Armenian hamster monoclonal α-CD11c IgG (clone N418), rat α-MHC class II IgG2b (clone NIMR-4), and Armenian hamster IgG isotype control were purchased from eBioscience (San Diego, CA, USA). Rat α-CD11c IgG2a (clone 223H7) was from Medical & Biological Laboratories (Nagoya, Japan). Rat α-CD86 IgG2b (clone 2D10) was from Southern Biotechnology Associates, Inc. (Birmingham, AL, USA). Rat α-CD16/CD32 IgG2b (clone 2.4G2) and isotype controls of rat IgG2a and rat IgG2b were from BD Bioscience Pharmingen (San Diego, CA, USA). FITC-labeled α-CD11c (α-CD11c-FITC, clone N418) was from miltenyi biotech (Bergisch Gladbach, Germany).

2.3.3. Quartz crystal microbalance (QCM)

The amount of IgGs bound to ZZ-BNCs was determined by a QCM model Twin-Q (As One Corp., Osaka, Japan), as described previously [24]. Briefly, the sensor chip of the QCM consisted of a 9-mm-diameter disk made from an AT-cut 27-MHz quartz crystal with gold electrodes on both sides (diameter, 2.5 mm; area, 4.9 mm^2). A frequency change (ΔF) of 1 Hz corresponded to a weight change of 0.6 ng/cm^2. The temperature of the measuring bath (~600 μl) was kept at 25°C. The bath was mixed at 600 rpm with a stirring tube. Measurements were taken in triplicate until a stable frequency (less than ± 3 Hz) was observed for >1 min. Protein sample were dissolved in 500 μl of PBS (phosphate-buffered saline). The sensor chip was treated with ZZ-BNC (4 μg/ml as protein), blocked with Block Ace (2 mg/ml, DS Pharma Biomedical, Osaka, Japan), and then reacted with each IgG isotype control (40 μg/ml).

2.3.4. Preparation of α-DC-ZZ-BNC complexes

Display of α-DC IgGs on the surface of ZZ-BNCs was carried out by chemical crosslinking as described previously [27]. Briefly, 1 μg of each IgG was crosslinked with Cy5- or CF750-labeled ZZ-BNCs (5 μg as protein) in the presence of 50 μM BS^3 (bis-sulfosuccinimidyl suberate, Pierce). After incubation at room temperature for 1 h, 100 μM glycine (pH 7.5) was added to quench the crosslinking reaction.

2.3.5. Ex vivo attachment assay to splenic DCs

Splenic DCs were isolated from BALB/c female mice (6-8 weeks, Japan SLC, Shizuoka, Japan). Briefly, spleens were treated with a gentleMACS dissociator (miltenyi biotech) in the presence of 2 mg/ml collagenase D (Roche, Mannheim, Germany). $CD11c^+$ cells were purified from the splenocytes by magnetic cell sorting

with MACS (miltenyi biotech) using FcR Blocking Reagent and α-CD11c (clone N418)-labeled magnetic beads. The cell population containing >80% $CD11c^+$ cells was used as splenic DCs for further experiments. DCs (2.5-5.0 × 10^5 cells) were mixed with each Cy5-labeled α-DC-ZZ-BNC complex (1 μg as ZZ-L protein), incubated at 4°C for 30 min, and then analyzed with a flow cytometer BD FACS Canto II (BD Biosciences, San Jose, CA, USA) with linear amplification for forward/side scatter and logarithmic amplification for FITC and Cy5 fluorescence. The FITC-derived fluorescence (emission 520 nm) was excited by a 488-nm laser and Cy5-derived fluorescence (emission 670 nm) was excited by a 633-nm laser.

2.3.6. In vivo imaging analysis

Each mouse was injected intravenously with 100 μl PBS containing 10 μg (as protein) of CF750-labeled ZZ-BNCs conjugated with each α-DC IgG. After 40 min, the mice were sacrificed, and the fluorescent signals for heart, lung, kidney, liver, and spleen were measured using an *in vivo* imaging system OV-100 (Olympus, Tokyo, Japan). The CF750-derived fluorescence (emission 777 nm) was excited with a xenon lamp and emission filter (from 708- to 752-nm), and obtained through a 770-nm interference barrier filter. To semi-quantify the accumulation of CF750-labeled α-DC-ZZ-BNC complexes in each organ, fluorescent signals were measured using WASABI software (Hamamatsu Photonics, Shizuoka, Japan).

2.3.7. In vivo attachment assay to splenic DCs

Cy5-labeled α-DC-ZZ-BNC complexes (10 μg as ZZ-L protein) were injected into mice intravenously. After 40 min, the mice were sacrificed and splenocytes were dissociated in MACS buffer with a gentleMACS dissociator. An aliquot (190 μl) of

cell suspension (2.0-5.0 × 10^6 cells) was mixed with 10 μl of α-CD11c-FITC, incubated at 4 °C for 30 min, and washed three times with MACS buffer. To evaluate the DC-targeting of each BNC, the cells were subjected to quantitative analysis by using a flow cytometer BD FACS Canto II with linear amplification for forward/side scatter and logarithmic amplification for FITC and Cy5 fluorescence. The subcellular localization of Cy5-labeled α-DC-ZZ-BNCs complexes was analyzed under a confocal laser scanning microscope (LSM) model FV-1000D (Olympus). Whole cell Z-stacks (each slice = 0.25 μm, total 15 sections) were acquired by LSM, which was equipped with a ×100 oil objective lens (Olympus).

2.3.8. Preparation of ZZ-BNC-LP complexes

ZZ-BNCs (100 μg as ZZ-L protein) were mixed with 600 μg of cationic LPs (cholesterol: dioleyl phosphatidylethanolamine (DOPE): o,o'-ditetradecanoyl-N-(α-trimethylammonioacetyl) diethanolamine chloride (DC-6-14) [28] = 3 : 3 : 4 (mol: mol: mol)) in Britton-Robinson buffer (pH 4), and incubated at 37°C for 30 min. The complexes of ZZ-BNCs with LPs (ZZ-BNC-LP complexes) were separated by CsCl isopycnic ultracentrifugation (5-40% (w/v)) in a P40ST rotor at 24,000 rpm at 25°C for 16 h. The amounts of ZZ-BNCs and LPs in each fraction (500 μl) were quantified with a BCA protein assay kit and a cholesterol E-test Wako kit (Wako), respectively. Fractions containing ZZ-BNC-LP complexes were combined and dialyzed against PBS at 4°C for overnight.

2.3.9. Immunization of mice with α-CD11c-ZZ-BNC-LP complexes containing JEV envelope-derived D3 Ag

JEV envelope-derived D3 Ag was expressed in Escherichia coli and purified as

described previously [29]. The D3 Ag (60 μg) was mixed with ZZ-BNC-LP complexes (120 μg of ZZ-L protein, 404 μg of LPs), incubated at room temperature for 1 h, and then 24 μg of α-CD11c antibodies (clone N418) was conjugated onto the surface of ZZ-BNC-LP-D3 complexes (see section 2.4.). An aliquot of α-CD11c-ZZ-BNC-LP-D3 complexes (20 μg as D3 Ag) was administrated to each mouse (BALB/c female, 7 weeks, Japan SLC) intravenously. After 4 weeks, booster immunization was carried out with α-CD11c-ZZ-BNC-LP-D3 complexes (20 μg as D3 Ag). Blood samples were collected from the tail vein for determination of serum α-D3 IgGs at 4 and 6 weeks after the first immunization.

2.3.10. ELISA (enzyme-linked immunosorbent assay) for serum α-D3 IgGs

The titers of serum α-D3 IgGs were measured by indirect ELISA as described previously [29]. Briefly, 96-well microtiter plates (Nalge Nunc International, Rochester, NY, USA) were coated with 1 μg/well of the E. coli-expressed recombinant D3 protein, and blocked with 10% (w/v) skimmed milk in bicarbonate buffer. Serially diluted antisera and horseradish peroxidase (HRP)-conjugated rabbit anti-mouse IgG (1:4000, Sigma-Aldrich, St. Louis, MO, USA) were added to wells, followed by HRP substrate. After 20 min of incubation at room temperature, the reaction was stopped by adding 1N sulfuric acid, and the absorbance was measured at 450 nm (OD_{450}) using a microplate reader (Bio-Rad Laboratories, Redmond, WA, USA).

2.4. Results and discussion

2.4.1. Preparation of α-DC-ZZ-BNCs

For efficient DC-targeting of ZZ-BNCs, I examined which commercial α-DC antibodies (*i.e.*, α-CD11c (2 clones), α-MHC class II, α-CD86, α-CD16/CD32, α-DC-SIGN (2 clones), α-CD207 (langerin, 2 clones)) could detect splenic DCs ($CD11c^+$ population of mouse splenocytes) by flow cytometry. Five of these antibodies (Armenian hamster monoclonal α-CD11c IgG (clone N418), rat α-CD11c IgG2a (clone 223H7), rat α-MHC class II IgG2b (clone NIMR-4), rat α-CD86 IgG2b (clone 2D10), rat α-CD16/CD32 IgG2b (clone 2.4G2)) were found to label splenic DCs more efficiently than the others. When the amounts of IgGs bound to ZZ-BNCs were determined by QCM [24], Armenian hamster IgGs were observed to be bound to ZZ-BNCs with high affinity (0.38 ± 0.07 mol per 1 mol ZZ-L protein), and rat IgG2a and IgG2b were weakly bound to ZZ-BNCs (0.02 ± 0.01 and 0.04 ± 0.02 mol per 1 mol ZZ-L protein, respectively). For the generation of stable α-DC-ZZ-BNC complexes, the chemical crosslinker BS^3 was added to the mixture of ZZ-BNCs and α-DC antibodies as described previously [27]. As shown in Table 2.1, the Z-averages and ζ-potentials of each α-DC-ZZ-BNC complex were less than 100 nm and negatively charged, respectively, suggesting that each α-DC-ZZ-BNC complex is suitable for *in vivo* targeting following systemic administration [30].

Table 2.1 Z-averages and ζ-potentials of α-DC-ZZ-BNC complexes.

BNCs	Antibodies	Z-averages (nm)	ζ-potentials (mV)
ZZ-BNC	None	51.1 ±0.2	-13.1 ±3.1
	α-CD11c (clone N418)	66.4 ±3.8	-20.3 ±1.5
	α-CD11c (clone 223H7)	52.2 ±0.1	-18.9 ±4.5
	α-MHC class II	54.3 ±1.1	-17.5 ±2.3
	α-CD86	54.4 ±1.5	-14.9 ±1.7
	α-CD16/CD32	51.7 ±0.4	-14.9 ±1.0
	Mouse total IgG	152 ±8.3	-25.2 ±0.8
BNC	-	69.0 ±0.2	-14.9 ±1.3

NOTE: Measurements were performed in triplicate. Values are indicated as mean ± SD.

2.4.2. Ex vivo attachment of α-DC-ZZ-BNCs to splenic DCs

Recently, our group demonstrated that fluorophore-labeled ZZ-BNC complexes are versatile bio-imaging probes for immunocytochemical analyses, which can display IgG Fv regions outwardly for the effective binding of Ags [24, 27]. Cy5-labeled ZZ-BNCs were mixed with each of five α-DC antibodies, crosslinked with BS^3, and added to the suspension of splenic DCs. Flow cytometric analyses showed that ZZ-BNCs displaying α-CD11c antibodies (clone N418) and α-MHC class II antibodies could accumulate onto 86% and 84% of splenic DCs, respectively (Fig. 2.2A). Other α-DC antibodies unexpectedly showed lower extents of accumulation, which were similar to those of mouse IgGs and ZZ-BNC alone, but higher than that of BNC alone. These results were confirmed from the mean fluorescent intensities of DCs incubated with each Cy5-labeled α-DC-ZZ-BNC complex (Fig. 2.2B). The difference in DC accumulation among the α-DC antibodies may be caused by either the number of antibodies on ZZ-BNC, or the affinity of each antibody to DCs. Because cell surface molecules on splenic DCs show high affinity to IgGs and ZZ domains [31-33], ZZ-BNCs displaying mouse IgGs and ZZ-BNC alone may accumulate on DCs. Furthermore, since BNCs and ZZ-BNCs possess high-mannose sugar chains [17], the mannose receptors of DCs may contribute to the interaction with them [34].

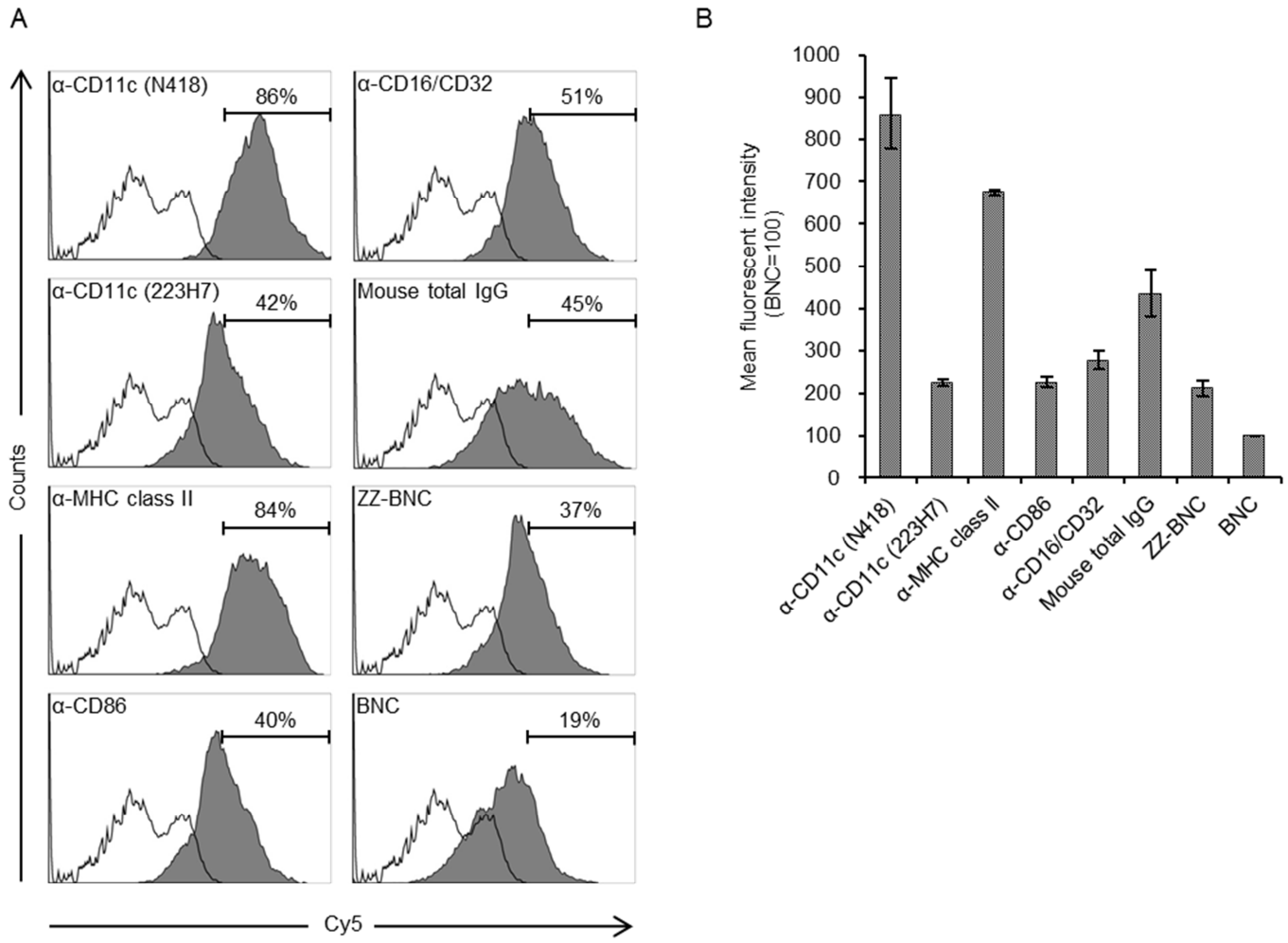

Fig. 2.2 Flow cytometric analysis of *ex vivo* attachment of α-DC-ZZ-BNCs complexes to splenic DCs.
(A) Accumulation of Cy5-labeled α-DC-ZZ-BNC complexes to isolated splenic DCs. Splenic DCs were incubated with each Cy5-labeled α-DC-ZZ-BNC complex and subjected to flow cytometric analysis. Fractions of DCs were pre-defined by the forward scatter/side scatter dot plots derived from $CD11c^+$ cells. Distributions of Cy5-derived fluorescence in ZZ-BNC-incubated DCs and untreated DCs are indicated as closed and open histograms, respectively. Antibodies against DCs are shown in the upper left of each panel. The percentages (%) of $ZZ\text{-}BNC^+$ cells in DCs are indicated as numbers. (B) Mean fluorescent intensities of the Cy5-labeled α-DC-ZZ-BNC complexes in DCs. Mean fluorescent intensity derived from DCs incubated with Cy5-labeled BNCs was defined as 100.
NOTE: Measurements were performed in triplicate. Error bars represent the SD.

2.4.3. In vivo distribution of α-DC-ZZ-BNCs

ZZ-BNCs displaying α-CD11c (clone N418) or α-MHC class II antibodies were labeled with CF750 and injected into the tail vein of mice (about 10 μg as ZZ-L protein per mouse). Because CF750-labeled α-DC-ZZ-BNC complexes were excreted into the bladder within 10 min of injection, it was judged that the complexes have circulated throughout the whole body by 40 min after injection. Mice were sacrificed at 40 min after injection and subjected to the extirpation of heart, lung, kidney, liver, and spleen. Each organ was observed for CF750-derived fluorescence on an OV-100 *in vivo* imaging system. As shown in Fig. 2.3A, both ZZ-BNCs and BNCs were found to localize in liver and spleen preferentially. Because spleen contains a larger number of lymphoid resident DCs than liver, and because splenic DCs can induce higher immune responses against exogenous Ags than hepatic DCs [35], I selected splenic DCs as a target of α-DC-ZZ-BNC for further study. Among the CF750-labeled α-DC-ZZ-BNC complexes, α-CD11c (clone N418) antibodies delivered CF750-labeled ZZ-BNCs to spleen with highest specificity (Figs. 2.3B and C). Mouse total IgGs, α-MHC class II antibodies and ZZ domains could also deliver CF750-labeled ZZ-BNCs to spleen to some extent, suggesting that these molecules have an affinity to splenic DCs as described above [31-33].

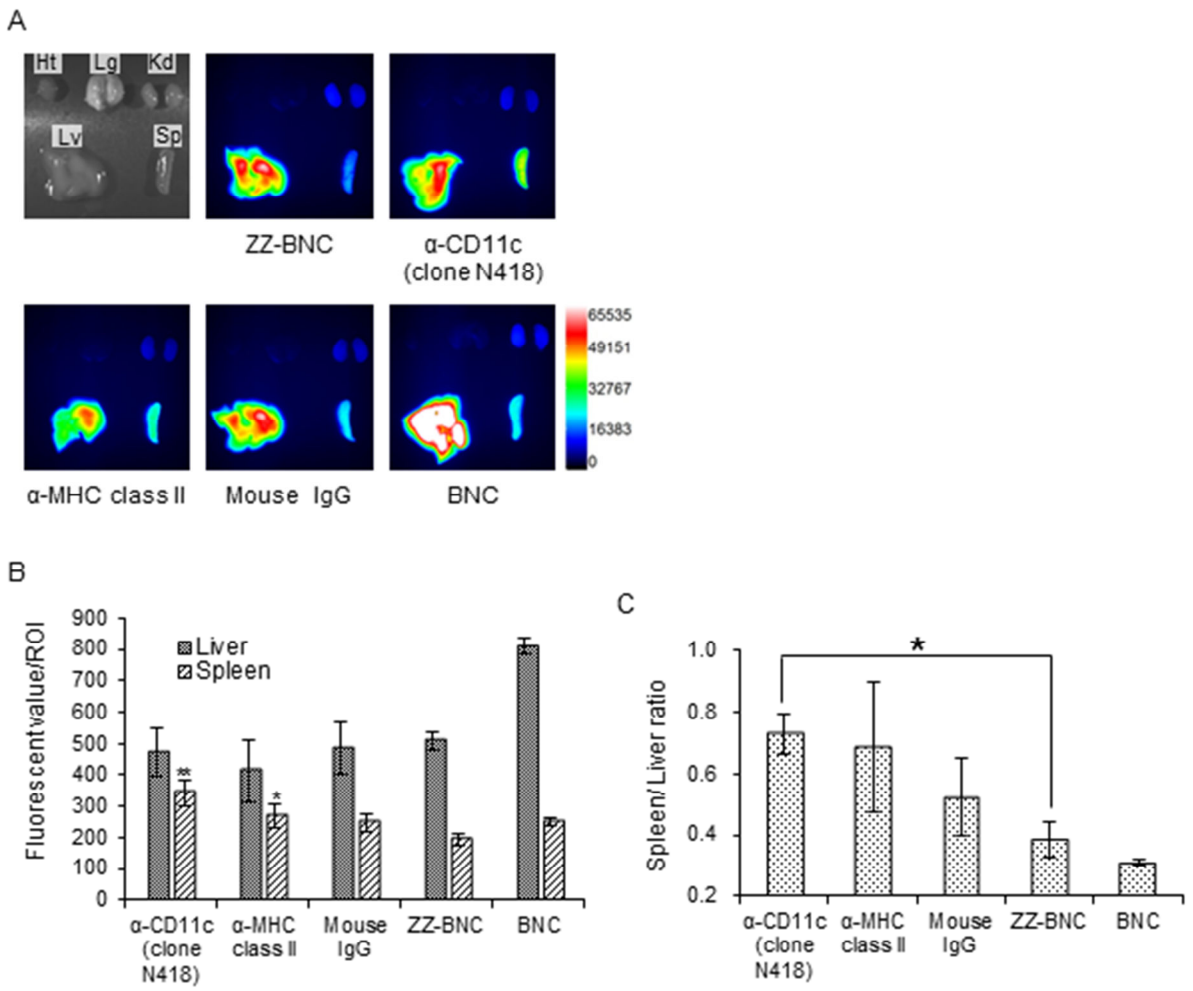

Fig. 2.3 *In vivo* distribution of CF750-labeled α-DC-ZZ-BNC complexes following IV injection into mice.
(A) CF750-derived fluorescence in each extirpated organ was observed using an OV-100 *in vivo* imaging system 40 min after IV injection to mice. (B) Fluorescent values of each organ in ROI were analyzed by WASABI software. Measurements were performed in triplicate. Error bars, SD; **, $p<0.01$; *, $p<0.05$. (C) Fluorescent ratio between spleen and liver in ROI was calculated from average fluorescent values of spleen and liver. *, $p<0.05$.
Abbreviations: heart, Ht; lung, Lg; kidney, Kd; liver, Lv; spleen, Sp; ROI, region of interest.

2.4.4. In vivo attachment of α-DC-ZZ-BNCs to splenic DCs

The Cy5-labeled ZZ-BNCs displaying α-CD11c (clone N418) antibodies, α-MHC class II antibodies, and mouse total IgGs were injected into mice intravenously (about 10 μg as ZZ-L protein per mouse). At 40 min after injection, mice were sacrificed and their spleens were extirpated. The splenocytes were isolated using a gentleMACS dissociator and analyzed by flow cytometry (Fig. 2.4A). The Cy5-labeled α-CD11c (clone N418)-ZZ-BNC complexes were detected in about 62% of $CD11c^+$ splenocytes, while the other Cy5-labeled ZZ-BNC complexes, Cy5-labeled ZZ-BNCs, and Cy5-labeled BNCs, were detected in a lower population of $CD11c^+$ splenocytes. Moreover, since Cy5-labeled α-CD11c (clone N418)-ZZ-BNC complexes were detected in 2.0% of $CD11c^-$ splenocytes (Fig. 2.4B), it is found that the complexes have high specificity to splenic $CD11c^+$ cells *in vivo*. Next, $CD11c^+$ cells were purified from the splenocytes by magnetic cell sorting with MACS using α-CD11c-labeled magnetic beads, stained immunocytochemically with FITC-labeled α-CD11c antibodies, and then observed under LSM (Fig. 2.5). ZZ-BNCs were colocalized with 82.4% ± 10.6% (mean ± SD, N = 73) of $CD11c^+$ cells. Z-stack projections of $CD11c^+$ cells containing ZZ-BNCs were generated from deconvolved slices using the maximum intensity criteria, indicating that the intravenously injected α-CD11c (clone N418)-ZZ-BNC complexes were immediately incorporated into splenic DCs.

When lymphocytic choriomeningitis viral vectors were injected into mice intravenously, viral particles accumulated to 11% and 60% of splenic DCs on days 3 and 7 after injection [8]. LPs displaying bacterial flagellin-related peptide could accumulate to about 20% of splenic DCs 1 h after IV injection [14]. Moreover, α-CD11c $F(ab)_2$-fused Ags could accumulate to 1.5% and 81.4% of splenic DCs at 4

and 12 h after SC injection [13]. These results demonstrated that the α-CD11c-ZZ-BNC complexes could more promptly and efficiently accumulate to splenic DCs (to 62% of $CD11c^+$ splenocytes at 40 min after IV injection) than other DC-targeting nanocarriers. Because ZZ-BNCs could display antibodies in an oriented-immobilization manner and thereby significantly enhance the sensitivity, Ag-binding capacity and affinity of the antibody itself [24, 26, 27], complex formation by α-CD11c antibodies with ZZ-BNCs may improve the molecular recognition between CD11c molecules and DC-targeting nanocarriers.

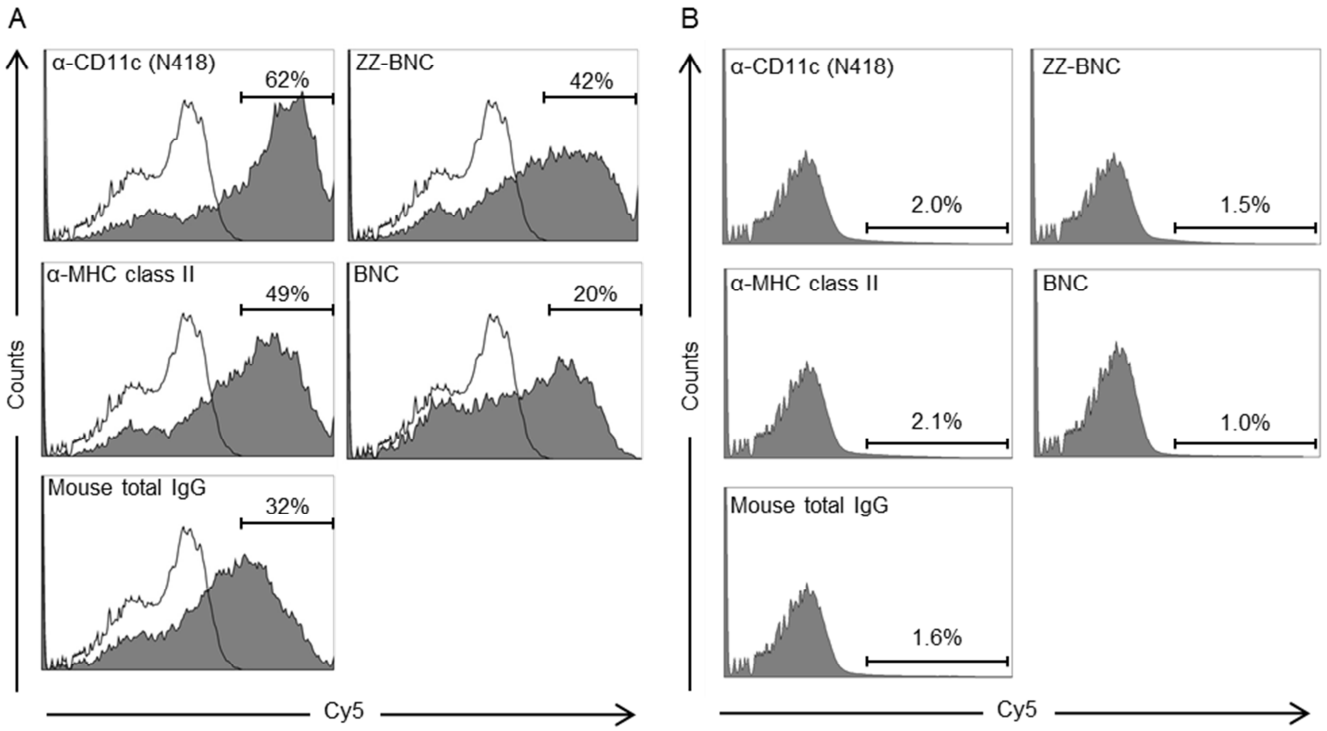

Fig. 2.4 Flow cytometric analysis of *in vivo* attachment of α-DC-ZZ-BNCs complexes to splenic DCs.
(A) Distributions of Cy5-derived fluorescence in splenic DCs isolated from Cy5-labeled α-DC-ZZ-BNC complex-injected mice and untreated mice are indicated by closed and open histograms, respectively. (B) Distributions of Cy5-derived fluorescence in splenic CD11c$^-$ cells isolated from Cy5-labeled α-DC-ZZ-BNC complex-injected mice.
NOTE: The percentages (%) of ZZ-BNC$^+$ cells in DCs and CD11c$^-$ cells are indicated as numbers.

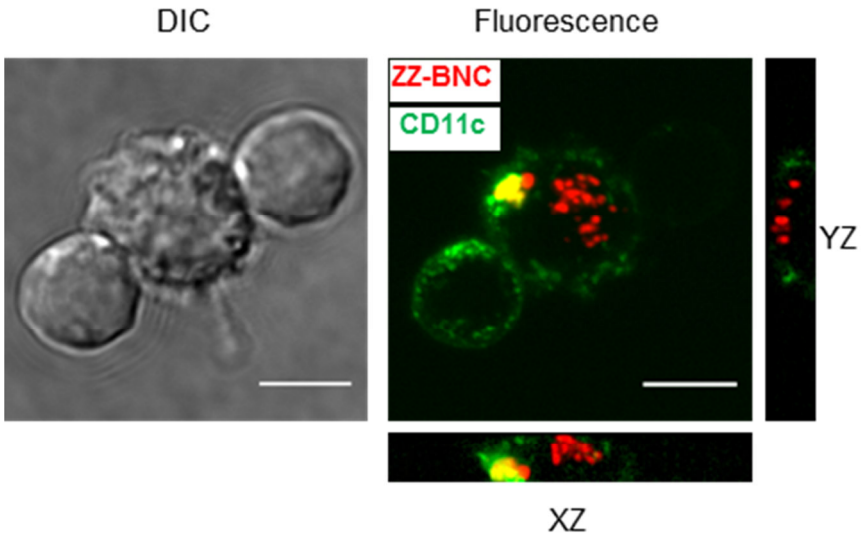

Fig. 2.5 Incorporation of Cy5-labeled α-CD11c (clone N418)-ZZ-BNC complexes by splenic DCs isolated from Cy5-labeled α-DC-ZZ-BNC complex-injected mice.
Z-stack projections of splenic DCs were generated from deconvolved slices using the maximum intensity criteria. Fluorescence derived from ZZ-BNCs and CD11c molecules is indicated in red and green, respectively. Scale bars, 5 μm.

2.4.5. Immunization of mice with α-CD11c-ZZ-BNC-LP-D3 complexes

ZZ-BNCs injected intravenously did not affect the morphology and the cytokine secretions of mouse splenocytes significantly (data not shown), which led me to examine the efficacy of the α-CD11c-ZZ-BNC complexes for delivering Ags to splenic DC cells *in vivo*. BNCs were shown to form a stable complex with LP spontaneously and deliver the complex in cell- and tissue-specific manner *in vivo* [21]. After mixing ZZ-BNCs with cationic LPs, the ZZ-BNC-LP complexes were purified by CsCl isopycnic ultracentrifugation, followed by dialysis against PBS. The complexes consisted of 19.5 μg/ml of ZZ-L protein and 65.6 μg/ ml of LPs, of which the Z-average (diameter) and ζ-potential were 426 nm (PDI, 0.331) and -5.76 mV, respectively. For evaluating *in vivo* delivery specifically to splenic DCs, I chose domain III (D3) of the JEV envelope protein as a control Ag. D3 Ag was expressed in *E. coli* and subsequently purified as described previously [29]. The ZZ-BNC-LP complex (120 μg as ZZ-L protein, 404 μg as LPs) was allowed to conjugate with 60 μg of D3 Ag by electrostatic interaction and to display 24 μg of α-CD11c antibodies (clone N418) on the complex. The Z-averages and ζ-potentials of α-CD11c-ZZ-BNC-LP-D3 complexes, ZZ-BNC-LP-D3 complexes, and LP-D3 complexes were 455 nm (PDI, 0.398), 324 nm (PDI, 0.261), and 106 nm (PDI, 0.130), and -9.53 mV, -1.87 mV, and 43.4 mV, respectively. While both the diameter and ζ-potential of α-DC-ZZ-BNC complexes were suitable for systemic administration, the conjugation with LPs increased their diameters to greater than 100 nm. However, because spleen can readily capture nanoparticles of more than 200 nm in diameter from the blood stream [36], it was considered that the α-CD11c-ZZ-BNC-LP-D3 complexes could deliver D3 Ags to splenic DCs efficiently following IV injection. Mice were immunized intravenously with α-CD11c (clone N418)-ZZ-BNC-LP-D3

complexes (20 μg as D3 Ag per each mouse) without adjuvant twice with a 4-week interval. D3 alone, LP-D3 complexes, and ZZ-BNC-LP-D3 complexes were used as control vaccines. These control vaccines containing 20 μg of D3 Ag were injected into each mouse in the same way. At 4 and 6 weeks after the first immunization, blood samples were collected from the tail vein for determination of serum α-D3 IgGs by ELISA (Fig. 2.6). At 4 weeks, no significant elicitation of α-D3 IgGs was observed in any mice. Only α-CD11c-ZZ-BNC-LP-D3 complexes elicited high titers of α-D3 IgGs at 6 weeks, while the other control vaccines containing the same amounts of D3 Ag did not. Considering that α-CD11c (clone N418)-ZZ-BNCs could accumulate in splenic DCs *in vivo* following IV injection (see Fig. 2.5), these results strongly suggested that α-CD11c-ZZ-BNC-LP complexes were able to effectively deliver D3 Ags to the inside of splenic DCs.

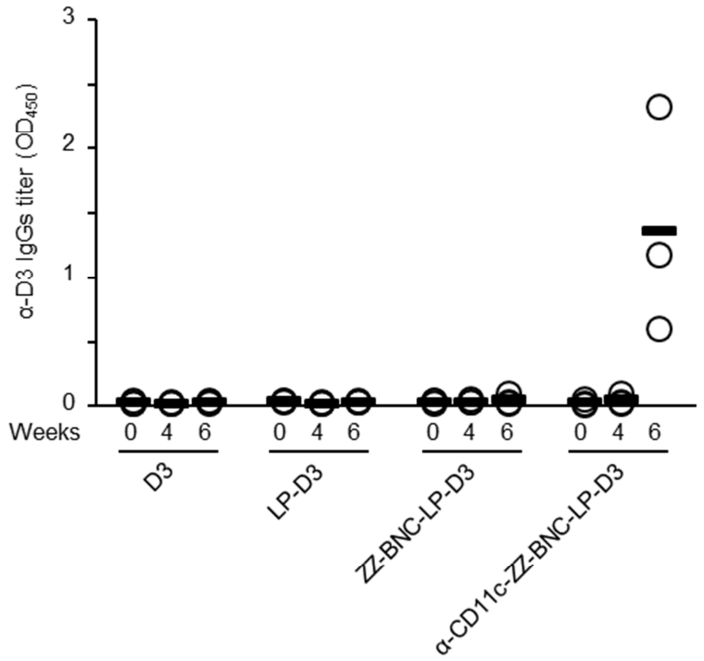

Fig. 2.6 Immunization of mice with α-CD11c-ZZ-BNC-LP-D3 complexes.
Titers of α-D3 IgG in sera collected from immunized mice at 0, 4 and 6 weeks were measured by ELISA. Measurements were performed in triplicate. Thick lines indicate average titers from each group.

Several lines of evidence have recently accumulated to indicate that DC targeting mediated by CD11c is superior to that mediated by other molecules. In human monocytes including DCs, CD11c molecules form heterodimers with CD18 molecules, also known as complement receptor 4 (CR4) [37]. Because CR4 mediates phagocytosis, α-CD11c-ZZ-BNC complexes may facilitate the efficient uptake of D3 Ags by DCs, leading to the effective induction of an α-D3 immune response. Moreover, it has been reported that α-CD11c $F(ab)_2$-conjugated Ags accumulated in the splenic marginal zone following IV injection and then migrated into the splenic T cell-zone, while α-MHC class II $F(ab)_2$-conjugated Ags accumulated in the splenic B cell-zone [38]. This result strongly suggested that DCs in the splenic marginal zone were stimulated with Ags in a CD11c-dependent manner and then migrated into the splenic T cell-zone. Taken together, the α-CD11c-ZZ-BNC-LP-D3 complexes are postulated to accumulate in splenic DCs, stimulate DCs with D3 Ags, move DCs from the marginal zone to the T cell-zone, present fragments of D3 Ag with MHC molecules to T cells along with co-stimulating factors (*e.g.*, CD80, CD86), and then induce D3-dependent immune responses including production of α-D3 IgGs. As for the administration route, it is practically rare to administrate vaccines intravenously. I should evaluate if this vaccine platform could target migratory DCs (*e.g.*, Langerhans cells) in mice after IM and SC administration.

2.5. Conclusion

ZZ-BNC is a scaffold for displaying IgGs in an oriented-immobilization manner, thus enhancing the sensitivity, Ag-binding capacity and affinity of IgG itself. In this study, I evaluated ZZ-BNCs displaying α-CD11c antibodies (clone N418) for *in vivo* DC-targeting following IV injection in mice. The α-CD11c-ZZ-BNC complexes accumulated to about 62% of splenic DCs, and were incorporated by DCs immediately. The α-CD11c-ZZ-BNC complex is a useful probe for *in vivo* imaging of DCs. Furthermore, the α-CD11c-ZZ-BNC-LP complexes loaded with JEV D3 Ags could elicit α-D3 IgG more efficiently than other non-targeting control vaccines, suggesting that this DC-specific nanocarrier is promising for forthcoming vaccines.

2.6. References

1. E.S. Trombetta, I. Mellman, Cell biology of antigen processing *in vitro* and *in vivo*. Annu Rev Immunol. 23 (2005) 975-1028.
2. J. Banchereau, F. Briere, C. Caux, J. Davoust, S. Lebecque, Y. Liu, B. Pulendran, K. Palucka, Immunobiogy of dendritic cells, Immunology 18 (2000) 767–811.
3. J.A. Villadangos, P. Schnorrer, Intrinsic and cooperative antigen-presenting functions of dendritic-cell subsets *in vivo*. Nat Rev Immunol. 7 (2007) 543-555.
4. B.M.L. Albert, S.F.A. Pearce, L.M. Francisco, B. Sauter, P. Roy, R.L. Silverstein, N. Bhardwaj, Immature dendritic cells phagocytose apoptotic cells via $\alpha_v\beta_5$ and CD36, and cross-present antigens to cytotoxic T lymphocytes, J. Exp. Med. 188 (1998) 1359–1368.
5. K. Inaba, R.M. Steinman, Accessory cell-T lymphocyte interactions. Antigen-dependent and -independent clustering, J. Exp. Med. 163 (1986) 247-261.
6. L. Flatz, A.N. Hegazy, A. Bergthaler, A. Verschoor, C. Claus, M. Fernandez, L. Gattinoni, S. Johnson, F. Kreppel, S. Kochanek, M. van den Broek, A. Radbruch, F. Lévy, P.H. Lambert, C.A. Siegrist, N.P. Restifo, M. Löhning, A.F Ochsenbein, G.J. Nabel, D.D. Pinschewer, Development of replication-defective lymphocytic choriomeningitis virus vectors for the induction of potent $CD8^+$ T cell immunity, Nat. Med. 16 (2010) 339–345.
7. N. Sevilla, S. Kunz, a Holz, H. Lewicki, D. Homann, H. Yamada, et al., Immunosuppression and resultant viral persistence by specific viral targeting of dendritic cells, J. Exp. Med. 192 (2000) 1249–1260.

8. L. Cervantes-Barragan, R. Züst, R. Maier, Dendritic cell-specific antigen delivery by coronavirus vaccine vectors induces long-lasting protective antiviral and antitumor immunity, MBio 1 (2010) e00171–10.

9. L. Yang, H. Yang, K. Rideout, T. Cho, K. il Joo, L. Ziegler, et al., Engineered lentivector targeting of dendritic cells for *in vivo* immunization, Nat. Biotechnol. 26 (2008) 326–334.

10. T. Uto, X. Wang, K. Sato, M. Haraguchi, T. Akagi, M. Akashi, M. Baba, Targeting of antigen to dendritic cells with poly(gamma-glutamic acid) nanoparticles induces antigen-specific humoral and cellular immunity, J. Immunol. 178 (2007) 2979–2986.

11. K.Y. Dane, C. Nembrini, A. a Tomei, J.K. Eby, C.P. O'Neil, D. Velluto, et al., Nano-sized drug-loaded micelles deliver payload to lymph node immune cells and prolong allograft survival, J. Control. Release 156 (2011) 154–160.

12. C.L. van Broekhoven, C.R. Parish, C. Demangel, W.J. Britton, J.G. Altin, Targeting dendritic cells with antigen-containing liposomes: a highly effective procedure for induction of antitumor immunity and for tumor immunotherapy, Cancer Res. 64 (2004) 4357–4365.

13. H. Wei, S. Wang, D. Zhang, S. Hou, W. Qian, B. Li, H. Guo, G. Kou, J. He, H. Wang, Y. Guo, Targeted delivery of tumor antigens to activated dendritic cells via CD11c molecules induces potent antitumor immunity in mice, Clin. Cancer Res. 15 (2009) 4612–4621.

14. A. Faham, J.G. Altin, Antigen-containing liposomes engrafted with flagellin-related peptides are effective vaccines that can induce potent antitumor immunity and immunotherapeutic effect, J. Immunol. 185 (2010) 1744–1754.

15. K.L. White, T. Rades, R.H. Furneaux, P.C. Tyler, S. Hook, Mannosylated liposomes as antigen delivery vehicles for targeting to dendritic cells, J. Pharm. Pharmacol. 58 (2006) 729–37.

16. T. Yamada, H. Iwabuki, T. Kanno, H. Tanaka, T. Kawai, H. Fukuda, A. Kondo, M. Seno, K. Tanizawa, S. Kuroda, Physicochemical and immunological characterization of hepatitis B virus envelope particles exclusively consisting of the entire L (pre-S1 + pre-S2 + S) protein, Vaccine 19 (2001) 3154–3163.

17. S. Kuroda, S. Otaka, T. Miyazaki, M. Nakao, Y. Fujisawa, Hepatitis B virus envelope L protein particles. Synthesis and assembly in *Saccharomyces cerevisiae*, purification and characterization, J. Biol. Chem. 267 (1992) 1953–1961.

18. J. Jung, M. Iijima, N. Yoshimoto, M. Sasaki, T. Niimi, K. Tatematsu, S.Y. Jeong, E.K. Choi, K. Tanizawa, S. Kuroda, Efficient and rapid purification of drug- and gene-carrying bio-nanocapsules, hepatitis B virus surface antigen L particles, from *Saccharomyces cerevisiae*, Protein Expr. Purif. 78 (2011) 149–155.

19. M. Yamada, A. Oeda, J. Jung, M. Iijima, N. Yoshimoto, T. Niimi, S.Y. Jeong, E.K. Choi, K. Tanizawa, S. Kuroda, Hepatitis B virus envelope L protein-derived bio-nanocapsules: Mechanisms of cellular attachment and entry into human hepatic cells, J. Control. Release 160 (2011) 322-329.

20. T. Yamada, Y. Iwasaki, H. Tada, H. Iwabuki, M.K.L. Chuah, T. VandenDriessche, H. Fukuda, A. Kondo, M. Ueda, M. Seno, K. Tanizawa, S. Kuroda, Nanoparticles for the delivery of genes and drugs to human hepatocytes, Nat. Biotechnol. 21 (2003) 885–890.

21. J. Jung, T. Matsuzaki, K. Tatematsu, T. Okajima, K. Tanizawa, S. Kuroda, Bio-nanocapsule conjugated with liposomes for *in vivo* pinpoint delivery of various materials., J. Control. Release 126 (2008) 255–264.

22. B. Nilsson, T. Moks, B. Jansson, L. Abrahmsén, A. Elmblad, E. Holmgren, C. Henrichson, T.A. Jones, M. Uhlén. A synthetic IgG-binding domain based on staphylococcal protein A. Protein Eng. 1 (1987) 107-113.

23. N. Kurata, T. Shishido, M. Muraoka, T. Tanaka, C. Ogino, H. Fukuda, A. Kondo, Specific protein delivery to target cells by antibody-displaying bionanocapsules, J. Biochem. 144 (2008) 701–707.

24. M. Iijima, H. Kadoya, S. Hatahira, S. Hiramatsu, G. Jung, A. Martin, J. Quinn, J. Jung, S.Y. Jeong, E.K. Choi, T. Arakawa, F. Hinako, M. Kusunoki, N. Yoshimoto, T. Niimi, K. Tanizawa, S. Kuroda, Nanocapsules incorporating IgG Fc-binding domain derived from *Staphylococcus aureus* protein A for displaying IgGs on immunosensor chips, Biomaterials 32 (2011) 1455–1464.

25. Y. Tsutsui, K. Tomizawa, M. Nagita, H. Michiue, T. Nishiki, I. Ohmori, M. Seno, H. Matsui, Development of bionanocapsules targeting brain tumors, J. Control. Release 122 (2007) 159–164.

26. M. Iijima, T. Matsuzaki, H. Kadoya, S. Hatahira, S. Hiramatsu, G. Jung, K. Tanizawa, S. Kuroda, Bionanocapsule-based enzyme-antibody conjugates for enzyme-linked immunosorbent assay, Anal. Biochem. 396 (2010) 257–261.

27. M. Iijima, T. Matsuzaki, N. Yoshimoto, T. Niimi, K. Tanizawa, S. Kuroda, Fluorophore-labeled nanocapsules displaying IgG Fc-binding domains for the simultaneous detection of multiple antigens, Biomaterials 32 (2011)

9011–9020.

28. A. Kikuchi, Y. Aoki, S. Sugaya, T. Serikawa, K. Takakuwa, K. Tanaka, N. Suzuki, H. Kikuchi, Development of novel cationic liposomes for efficient gene transfer into peritoneal disseminated tumor, Hum. Gene Ther. 10 (1999) 947–955.

29. S. Tafuku, T. Miyata, M. Tadano, R. Mitsumata, H. Kawakami, T. Harakuni, T. Sewaki, T. Arakawa, Japanese encephalitis virus structural and nonstructural proteins expressed in *Escherichia coli* induce protective immunity in mice, Microbes Infect. (2011) 4–11.

30. S.M. Moghimi, A.C. Hunter, J.C. Murray, Long-circulating and target-specific nanoparticles: theory to practice, Pharmacol. Rev. 53 (2001) 283–318.

31. J.M.H. de Jong, D. Schuurhuis, A. Ioan-Facsinay, E.I.H. van der Voort, T.W.J. Huizinga, F. Ossendorp, R.E. Toes, J.S. Verbeek, Murine Fc receptors for IgG are redundant in facilitating presentation of immune complex derived antigen to $CD8^+$ T cells *in vivo*, Mol. Immunol. 43 (2006) 2045–2050.

32. B. Fournier, D.J. Philpott, Recognition of *Staphylococcus aureus* by the innate immune system, Clin. Microbiol. Rev. 18 (2005) 521-540.

33. X. Ding, W. Yang, X. Shi, P. Du, L. Su, Z. Qin, J. Chen, H. Deng, TNF Receptor 1 Mediates Dendritic Cell Maturation and CD8 T Cell Response through Two Distinct Mechanisms, J. Immunol. 187 (2011) 1184–1191.

34. S. Burgdorf, V. Lukacs-kornek, C. Kurts, The mannose receptor mediates uptake of soluble but not of cell-associated antigen for cross-presentation, J. Immunol. 176 (2006) 6770-6776.

35. V.G. Pillarisetty, A.B. Shah, G. Miller, J.I. Bleier, R.P. DeMatteo, Liver

dendritic cells are less immunogenic than spleen dendritic cells because of differences in subtype composition, J. Immunol. 172 (2004) 1009–1017.

36. A.L. Klibanov, K. Maruyama, A.M. Beckerleg, V.P. Torchilin, L. Huang, Activity of amphipathic poly(ethylene glycol) 5000 to prolong the circulation time of liposomes depends on the liposome size and is unfavorable for immunoliposome binding to target, Biochim. Biophys. Acta. 1062 (1991) 142–148.

37. G.D. Keizer, A.A. Te Velde, R. Schwarting, C.G. Figdor, J.E. De Vries, Role of p150,95 in adhesion, migration, chemotaxis and phagocytosis of human monocytes, Eur. J. Immunol. 17 (1987) 1317–1322.

38. F.V. Castro, A.L. Tutt, A.L. White, J.L. Teeling, S. James, R.R. French, M.J. Glennie, CD11c provides an effective immunotarget for the generation of both CD4 and CD8 T cell responses, Eur. J. Immunol. 38 (2008) 2263–2273.

Chapter III

Immunological analyses of DC-targeting bio-nanocapsule-based vaccine

3.1. Abstract

Active targeting of DCs has been considered promising to improve the immunogenicity of conventional subunit vaccines. While various nanocarriers (*e.g.*, LPs, nanomicelles, nanogels) have been utilized for DC-specific Ag delivery, effective innate immunity could not be elicited by their own, presumably due to the lack of DC priming ability. Recently, our group has established BNC, a HBV surface Ag L protein particle, as a nanocarrier harboring machineries for viral infection and *in vivo* targeting. BNCs have been modified to display tandem form of IgG Fc-binding Z domain (ZZ-BNC), and then conjugated with α-CD11c IgGs to form α-DC-ZZ-BNC complex. Through IV injection, the α-DC-ZZ-BNCs could accumulate into splenic DCs promptly and efficiently, and the complex with Ag-loaded cationic LPs (α-DC-ZZ-BNC-LP-Ag) by itself could elicit effective Ag-specific IgG production. In this study, although the α-DC-ZZ-BNC injected locally (intramuscularly, subcutaneously) could accumulate into approximately 10% of DCs in LN closest to injection site, the α-DC-ZZ-BNC-LP-Ag injected locally was less effective, of which the positive charge may disturb the accumulation into DCs in draining LNs. To optimize the particle properties for local administrations, instead of liposomal fusion, the surface of α-DC-ZZ-BNC was chemically modified with Ags (α-DC-ZZ-BNC-Ag). Even in the absence of adjuvants, the α-DC-ZZ-BNC-Ag could be incorporated by DCs efficiently, leading to effective DC maturation, T cell responses, and Ag-specific

IgG productions. Moreover, the α-DC-ZZ-BNC modified with JEV envelope-derived D3 Ags by itself could confer protection against 50-fold lethal dose of JEV on mice. Collectively, the α-DC-ZZ-BNC-Ag platform was shown to be a promising DC-targeting technology for forthcoming vaccines.

3.2. Introduction

Subunit vaccines have been utilized for avoiding the side-effects of conventional vaccines (*e.g.*, live, live-attenuated, inactivated vaccines), whereas low immunogenicity often observed in subunit vaccines has remained to be solved. DDS-based subunit vaccines, delivering Ags to APCs efficiently, have therefore become promising for enhancing the immunogenicity of conventional subunit vaccines. Especially, since DCs play a pivotal role in adaptive immunity, various nanocarriers (*e.g.*, LPs, micelles, nanogels) have been targeted to DCs by displaying molecules recognizing with DC-specific receptors (integrin [1, 2], C-type lectin [3-6], and Fc receptors [7, 8]), and thereby these nanocarriers have shown to enhance the immunogenicity of loaded Ags *in vivo* [9, 10]. Meanwhile, it has been known that priming of innate immunity is necessary for eliciting following adaptive immunity [11]. Due to the less stimulatory effect on pattern recognition molecules (PRRs) including Toll-like receptors of these nanocarriers, while it should be revealed how adjuvants enhance innate immunity on the molecular basis for their safety, these nanocarriers require additional adjuvants consisting of their ligands [12]. Furthermore, the intracellular kinetics of delivered Ags in DCs should be controlled for eliciting effective humoral and cellular immunities. Incorporated Ags in endosomes are processed to small peptides for presenting to naïve $CD4^+$ T cells via major histocompatibility complex (MHC) class II, leading to the initiation of helper T cell (Th cell)-dependent immunity (*i.e.*, humoral immunity). On the other hands, a part of incorporated Ags are translocated from endosome to cytoplasm, processed to small peptides, and then transferred to endoplasmic reticulum for presenting to naïve $CD8^+$ T cells via MHC class I, leading to the initiation of cytotoxic T lymphocyte (CTL)-dependent immunity (*i.e.*, cellular immunity) [13, 14]. For example, the

Ag-encapsulated LPs consisting of pH-sensitive fusogenic polymer could release Ags efficiently to cytoplasm by endosomal membrane fusion under acidic condition in late-endosome, which elicits more effective CTL activity rather than original LPs [15]. Thus, DC-targeting nanocarriers should control intracellular kinetics of Ags in DCs to induce the most effective immune responses against each pathogen. Generally, prophylactic vaccine is essentially based on humoral immunity, contributing to neutralizing pathogens, facilitating phagocytosis, and complement fixation. In contrast, therapeutic vaccine is mainly based on cellular immunity, eliminating pathogens and infected cells [16, 17].

BNC is an approximately 50-nm hollow nanoparticle consisting of HBV surface Ags L proteins, which could be synthesized up to approximately 40% (w/w) of total soluble proteins in recombinant yeast cells [18, 19]. Since N-terminal region of L protein harbors HBV-derived human liver-specific recognition domain and membrane fusogenic domain, BNCs could function as a nanocarrier specific to human hepatic cells with comparable infectivity of HBV [20, 21]. After fusion with LPs containing payloads (anionic LPs for proteins and compounds, cationic LPs for DNAs), BNC-LP complex could deliver them to human hepatic cells specifically [21, 22]. Moreover, our group generated mutated BNC (ZZ-BNC) by replacing human liver-specific recognition domain with a tandem form of IgG Fc-binding Z domain from *Staphylococcus aureus* protein A to display IgGs outwardly in an oriented immobilization manner [23-25]. Recently, I have developed DC-targeting BNCs by displaying α-CD11c IgGs (clone N418) on ZZ-BNC (α-DC-ZZ-BNC) [26]. Followed by the IV injection to mice, α-DC-ZZ-BNC was revealed to accumulate into approximately 62% of splenic DCs. After fusion with Ag-loaded cationic LPs (LP-Ag), the α-DC-ZZ-BNC-LP-Ag complex injected intravenously could efficiently induce

Ag-specific IgG production rather than Ag alone. Thus, α-DC-ZZ-BNC has advantages in DC-specific delivery of Ags for eliciting Ag-specific immunity effectively. Because vaccines have been injected through SC and IM routes at worldwide clinical sites, the SC-injected α-DC-ZZ-BNC-LP-Ag complex was found less immunogenic unexpectedly (Table 3.1, Fig. 3.1). Its positive charge (~27.9 mV) might disturb the movement of the complex from injection site to DCs, strongly suggesting that the complex is unsuitable for the DC-specific delivery through local injections. On the other hand, our group has recently developed a vaccine platform consisting of Ag-crosslinked ZZ-BNC [27]. When ZZ-BNC was chemically conjugated with JEV-derived D3 Ag, the ZZ-BNC-D3 complex injected through SC route could induce JEV-specific neutralizing IgG production more effectively than D3 alone in mice. These situations have led me to examine if the α-DC-ZZ-BNC-Ag complex induces more effective immunity than ZZ-BNC-Ag even through local injections.

In this study, I have formulated the α-DC-ZZ-BNC-Ag complex by using model Ag ovalbumin (OVA), and demonstrated that the complex could deliver Ags to DCs *ex vivo*. The complex was found to induce DC maturation without any adjuvant, followed by CTL proliferation and Th1/Th2 immune responses. Furthermore, for demonstrating that the complex is more effective platform for prophylactic vaccines than conventional vaccines, I examined the protective efficacy of α-DC-ZZ-BNC-D3 complex against JEV infection in mice.

Table 3.1 Particle properties of α-DC-ZZ-BNC-LP-D3 analyzed by a DLS.

Samples	Z-average (nm)	PDI	ζ-potential (mV)
LP-D3	44.7 ± 1.1	0.227 ± 0.02	47.2 ± 12
ZZ-BNC-LP-D3	84.3 ± 11	0.186 ± 0.02	30.4 ± 5.5
α-DC-ZZ-BNC-LP-D3	91.5 ± 9.2	0.203 ± 0.02	27.9 ± 4.0
IgG-ZZ-BNC-LP-D3	106 ± 23	0.298 ± 0.07	26.0 ± 5.2

Measurements were performed in triplicate. Values are indicated as mean ± SD.

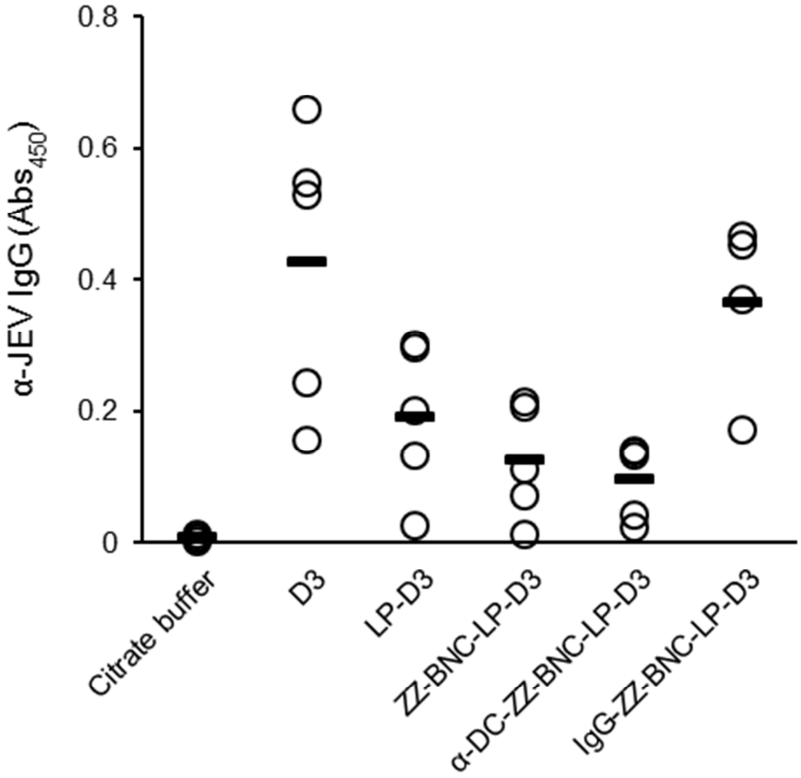

Fig. 3.1 Induction of JEV-specific IgGs production with α-DC-ZZ-BNC-LP-D3 complex.
Mice were received SC injection of α-DC-ZZ-BNC-D3 (30 μg as D3) at week 0, 2, and 4. Sera were collected from the immunized mice, and then titers of JEV-specific total IgG was determined by using ELISA. Measurements were performed with six mice in each group. Thick lines indicate average titers from each group.

3.3. Materials and Methods

3.3.1. Materials

Endotoxin-free OVA was purchased from Invivogen (Endofit OVA; San Diego, CA, USA). ZZ-BNCs were overexpressed in *Saccharomyces cerevisiae* AH22R$^-$ cells carrying ZZ-BNC-expression plasmid pGLD-ZZ50 [25], and purified as described previously [28]. Protein concentrations were determined with a micro BCA protein assay kit (Pierce, Rockford, IL, USA) using bovine serum albumin as a control protein. OVA was labeled with a CF488A maleimide (Biotium, Heyward, CA, USA) according to the manufacturer's protocol. BNC was also labeled with a CF633 NHS ester or a CF750 NHS ester (Biotium). FluoSphere (carboxylate-modified, 40 nm in diameter, yellow-green) was purchased from Life Technologies (Carlsbad, CA, USA). Z-averages and ξ-potentials of ZZ-BNCs were measured in water at 25℃ by a DLS model Zetasizer Nano ZS (Malvern Instruments, Worcestershire, UK).

3.3.2. Preparation of OVA-conjugated α-DC-ZZ-BNC

OVA was conjugated with ZZ-BNC by using two types of chemical crosslinker (Sulfo-LC-SPDP, sulfosuccinimidyl 6-[3´(2-pyridyldithio)-propionamido] hexanoate; SPDP, N-succinimidyl- 3-(2-pyridyldithio) propionate; Pierce) as described previously (Fig. 3.2A) [27]. Briefly, ZZ-BNCs (1 mg/ml as protein) and OVA (1 mg/ml) were reacted with Sulfo-LC-SPDP (500 μM) and SPDP (500 μM) to generate pyridyldithiol residues on each protein, respectively. Pyridyldithiol-activated OVA (10 mg/ml) was reduced with dithiothreitol (DTT; 50 mM) to generate sulfhydryl residues. Finally, pyridyldithiol-activated ZZ-BNCs (1 mg/ml as protein) and sulfhydryl-activated OVA (1 mg/ml) were mixed and then incubated at 4 ˚C for 18 h to allow the formation of

disulfide bonds. The OVA-conjugated ZZ-BNCs were designated as ZZ-BNC-OVA.

Either Armenian hamster monoclonal α-CD11c IgG (clone N418; eBioscience, San Diego, CA, USA) or Armenian hamster IgG isotype control (eBioscience) was displayed onto ZZ-BNC-OVA as described previously [29]. Briefly, α-CD11c IgG (1 μg) was mixed with ZZ-BNC-OVA (5 μg as ZZ-L protein) in the presence of 50 μM BS^3 (Pierce), and then incubated at room temperature for 1 h. Crosslinking reaction was stopped by the addition of glycine (pH 7.5, 100 μM, final concentration). The α-CD11c IgG-displayed ZZ-BNC-OVA was designated as α-DC-ZZ-BNC-OVA.

3.3.3. Ex vivo cellular uptake analysis of splenic DCs

The care of the animal and all of the experimental procedures used in these experiments were approved by the Committee on Animal Experiments of Graduate School of Bioagricultural Sciences, Nagoya University. Spleens were isolated from C57BL/6 mice (6 weeks, female, Japan SLC, Inc., Hamamatsu, Japan), and splenocytes were prepared with gentleMACS dissociator (Miltenyi Biotech, Bergisch Gladbach, Germany) in the presence of 2 mg/ml collagenase D (Roche, Mannheim, Germany). $CD11c^+$ cells were purified from the splenocytes by a magnetic-activated cell sorting (MACS, Miltenyi Biotech) using a FcR Blocking Reagent and an α-CD11c IgG (clone N418)-conjugated magnetic beads. The cell preparations containing >80% $CD11c^+$ cells were used as splenic DCs for further experiments. Splenic DCs (approximately 2.0×10^5 cells) were mixed with CF488A-labeled α-DC-ZZ-BNC-OVA (2 μg as OVA), incubated in RPMI1640 medium supplemented with 10% (v/v) FBS at 37℃ for 4 h under humidified 5% (v/v) CO_2 condition. The cells were washed with MACS buffer (Phosphate-buffered saline (PBS) containing 0.5% (w/v) BSA and 2 mM EDTA) analyzed by a flow cytometer BD FACS Canto II

(BD Biosciences, San Jose, CA, USA) with linear amplification for forward/side scatter and logarithmic amplification for CF488A fluorescence (excitation at 488 nm, emission at 515 nm). Splenic DCs loaded with CF488A-labeled α-DC-ZZ-BNC-OVA were stained with an wheat germ agglutinin Alexa Fluor 633 Conjugate (Life Technologies), and then observed under a confocal LSM model FV-1000D (Olympus, Tokyo, Japan). Whole cell Z-stacks (each slice = 0.5 μm, total 14 sections) were acquired by LSM, which was equipped with a ×100 oil objective lens (Olympus).

3.3.4. In vivo distribution analysis

CF750-labeled α-DC-ZZ-BNC (10 μg as ZZ-L protein) was injected to Balb/c mice (6-8 weeks, female, Japan SLC, Inc.) through SC or IM routes. After 12 h, the mice were sacrificed, and tissues (heart, lung, kidney, liver, spleen and LNs (inguinal, ILN; popliteal, PLN; axillary, ALN)) were isolated. Fluorescent signals in each tissue were observed by using an *in vivo* imaging system OV-100 (Olympus). Under the excitation with xenon lamp equipped with emission filter (from 708- to 752-nm), CF750-derived fluorescence (maximum emission, 777 nm) was obtained through 770-nm interference barrier filter, and then semi-quantified with an image processing program FV10-ASW version 4 (Olympus).

3.3.5. Analysis of in vivo accumulation to APCs in LNs

CF633-labeled α-DC-ZZ-BNC (10 μg as ZZ-L protein) was injected to Balb/c mice (6-8 weeks, female, Japan SLC, Inc.) through SC or IM routes. The mice were sacrificed at 8, 12, and 24 h after injection; LNs closest to injection sites were isolated, and then cells were released from LNs by homogenization with ground glasses. The cells were stained with FITC-labeled forms of α-CD11c IgG (α-CD11c-FITC;

Miltenyi Biotech), α-CD11b IgG (α-CD11b-FITC; Miltenyi Biotech), and α-CD19 IgG (α-CD19-FITC; Miltenyi Biotech). These cells were analyzed by using a flow cytometer with linear amplification for forward/side scatter and logarithmic amplification for FITC and CF633 fluorescence. The FITC-derived fluorescence (maximum emission, 515 nm) was excited by a 488-nm laser, and the CF633-derived fluorescence (maximum emission, 650 nm) was excited by a 633-nm laser.

3.3.6. Analysis of ex vivo DC maturation

Splenic DCs (approximately 5.0×10^5 cells) plated in 1 ml RPMI1640 medium supplemented with 10% FBS were incubated with 10 μg (as OVA) of OVA, ZZ-BNC-OVA, or α-DC-ZZ-BNC-OVA at 37 ˚C for 24 h under humidified 5% CO_2 condition. Lipopolysaccharides (LPS; 10 μg, Sigma Aldrich) were added to the medium for inducing DC maturation as a positive control. After 24 h incubation, the cells were collected with MACS buffer, and stained with APC-labeled forms of α-CD80 IgG (Miltenyi Biotech), α-CD86 IgG (Miltenyi Biotech), or α-CD40 IgG (Miltenyi Biotech). The APC-derived fluorescence (maximum emission, 660 nm) was analyzed by using a flow cytometer.

3.3.7. Analysis of in vivo OVA-specific T cell responses

After 7 days from SC injection of α-DC-ZZ-BNC-OVA (10 μg as OVA), C57BL/6 mice were sacrificed, and the spleens were applied to gentleMAC dissociator. The splenocytes were stained with APC-labeled H-$2k^b$ OVA tetramer-SIINFEKL (MBL, Nagoya, Japan) and FITC-labeled α-CD8 IgG (MBL) for detection of OVA-specific $CD8^+$ T lymphocytes. These cells were subjected to a flow cytometer for measuring APC- and FITC-derived fluorescence.

The splenocytes (approximately 2.0×10^6 cells) isolated from C57BL/6 mice injected with α-DC-ZZ-BNC-OVA were incubated in 1 ml RPMI1640 medium supplemented with 10% FBS and 40 μg OVA at 37 ˚C for 7 days under humidified 5% CO_2 condition. The IFN-γ concentrations of supernatants were quantified by using ELISA Ready-SET-Go! kit (eBioscience).

3.3.8. Analysis of in vivo OVA-specific IgG production

C57BL/6 mice (female, 6 weeks, Japan SLC, Inc.) were received SC injection of α-DC-ZZ-BNC-OVA (10 μg as OVA) at week 0, 2, and 4. Blood samples (about 50 μl) were collected from the tail vein at week 6, and allowed to form blood clots. Titers of OVA-specific IgGs (total IgG, IgG1, and IgG2a) in sera were determined by using ELISA. Briefly, each well of 96-well plates was coated with 50 μl of 20 μg/ml OVA in bicarbonate buffer (pH 9.6) at 4 ˚C for overnight, and blocked with 10% (w/v) skimmed milk (Wako, Osaka, Japan) at 37 ˚C for 2 h. Serially diluted sera (50 μl) were added to each well and incubated at 37 ˚C for 2 h. After washing with PBST (PBS containing 0.1% (v/v) Tween 20) three times and PBS three times, 200 ng/ml of HRP-conjugated secondary antibodies (α-mouse total IgG, Sigma Aldrich; α-mouse IgG1, eBioscience; or α-mouse IgG2a, Abcam, Cambridge, UK) were added to each well, and incubated at 37 ˚C for 2 h. After washing with PBST three times and PBS three times, 100 μl of 3,3'-5,5'-tetramethylbenzidine (TMB) substrate (Pierce) was added to each well, and incubated at room temperature for 20 min. The reaction was stopped by adding 50 μl of 2N sulfuric acid, and the absorbance was measured at 450 nm (OD_{450}). Based on the OD_{450} value of 100-fold diluted non-immune sera (n = 4), the cut-off value (COV) was defined as the mean of OD_{450} values plus 2-fold value of the standard deviation (SD); COV = [mean + (SD × 2)]. Titers of α-OVA IgGs were

defined as the highest serum dilution at which OD_{450} became closest to COV.

3.3.9. Protection assay with JEV D3-conjugated α-DC-ZZ-BNC

JEV envelope-derived D3 protein was expressed in *Escherichia coli* and purified as described previously [30]. D3 protein was conjugated to one-fourth weight (as ZZ-L protein) of α-DC-ZZ-BNC with SPDP and sulfo-LC-SPDP as described above. The D3-conjugated α-DC-ZZ-BNC (α-DC-ZZ-BNC-D3; 30 μg as D3 protein) was injected to Balb/c mice (7 weeks, female, Japan SLC, Inc.) through SC route at weeks 0, 2, and 4. After blood collection from tail vein at week 6, the mice were challenged intraperitoneally with 50-times dose of 50% lethal dose ($50LD_{50}$) of the JEV JaGAr01 strain followed by intracerebral inoculation with PBS. The mice were subjected to monitoring the signs of illness/distress such as ruffled fur or paralysis and recording the survival rates.

Titers of α-JEV IgGs (including α-D3 IgGs) in sera were determined by using ELISA as described previously [30]. Briefly, each well of 96-well plates was coated with 50% (v/v) Japanese Encephalitis TC Vaccine (Kaketsuken, Kumamoto, Japan) in bicarbonate buffer (pH 9.6) at 4 ˚C for overnight. Similar to the ELISA for OVA-specific IgG (see above), each well was blocked, contacted with sera, washed with PBST and PBS, contacted with HRP-conjugated α-mouse IgGs, and developed with TMB substrate. After measuring OD_{450} values, titers were calculated by the same method for OVA-specific IgG.

3.4. Results

3.4.1. Cellular uptake of α-DC-ZZ-BNC-OVA by splenic DCs

Due to the less immunogenicity of α-DC-ZZ-BNC-LP-Ag complex (*see* **3.2. Introduction**), model Ag (OVA) and ZZ-BNC were treated with SPDP and sulfo-LC-SPDP crosslinkers, respectively, and then mixed them to form OVA-crosslinked ZZ-BNC (ZZ-BNC-OVA) (Fig. 3.2A). Since efficient DC targeting of ZZ-BNC could be achieved by displaying α-CD11c IgGs [26], the ZZ-BNC-OVA complex was conjugated with α-CD11c IgGs, followed by the chemical treatment with BS^3. Based on the densitometric intensities of SDS-polyacrylamide gel electrophoresis analysis, the α-DC-ZZ-BNC-OVA complex was estimated to contain approximately 128 molecules of OVA and 8 molecules of α-CD11c IgG per 1 molecule of ZZ-BNC. As a non-targeting control, isotype IgG-displaying ZZ-BNC-OVA (IgG-ZZ-BNC-OVA) complex was prepared similarly. As a ZZ domain-less control, BNC (an original form) was conjugated with OVA to form BNC-OVA complex. As shown in Table 3.2, diameter of each complex is less than 100 nm and negatively charged (~ -30 mV), which were considered suitable for Ag-delivery to DCs in lymph organs and injection sites [31].

After incubation of isolated splenic DCs with CF488-labeled OVA-crosslinked α-DC-ZZ-BNC (α-DC-ZZ-BNC-fOVA) at 37 °C for 4 h, flow cytometric analysis demonstrated that fOVA was accumulated to 67% of DCs, while fOVA alone, BNC-fOVA, ZZ-BNC-fOVA, and IgG-ZZ-BNC-fOVA to 6.0%, 9.1%, 14%, and 15% of DCs, respectively (Fig. 3.2B). Mean fluorescent intensity of α-DC-ZZ-BNC-fOVA was approximately 12-fold, 4.5-fold, and 5.9-fold higher than those of fOVA alone, ZZ-BNC-fOVA, and IgG-ZZ-BNC-fOVA, respectively. These results indicated that

the conjugation with α-CD11c IgGs could confer DC-targeting capability on ZZ-BNC-OVA. Furthermore, it was suggested that both ZZ domains and high mannose-type sugar chains of ZZ-BNC help the accumulation to DCs by interacting with Ig molecules and mannose receptors on the cell surface, respectively [13]. Next, the fluorescence of α-DC-ZZ-BNC-fOVA in DCs was observed under laser scanning microscopy. As shown in Fig. 3.2C, fOVA was localized inside of DCs, indicating that α-DC-ZZ-BNC-fOVA could deliver fOVA to the intracellular fraction of DCs efficiently.

Table 3.2 Particle properties of α-DC-ZZ-BNC-OVA analyzed by a DLS.

Samples	Z-average (nm)	PDI	ζ-potential (mV)
BNC-OVA	91.5 ± 1.1	0.236 ± 0.01	-33.3 ± 4.1
ZZ-BNC-OVA	68.0 ± 8.2	0.236 ± 0.04	-30.2 ± 1.7
α-DC-ZZ-BNC-OVA	68.2 ± 9.7	0.215 ± 0.04	-27.9 ± 4.0
IgG-ZZ-BNC-OVA	80.9 ± 20	0.222 ± 0.04	-26.3 ± 6.8

Measurements were performed in triplicate. Values are indicated as mean ± SD.

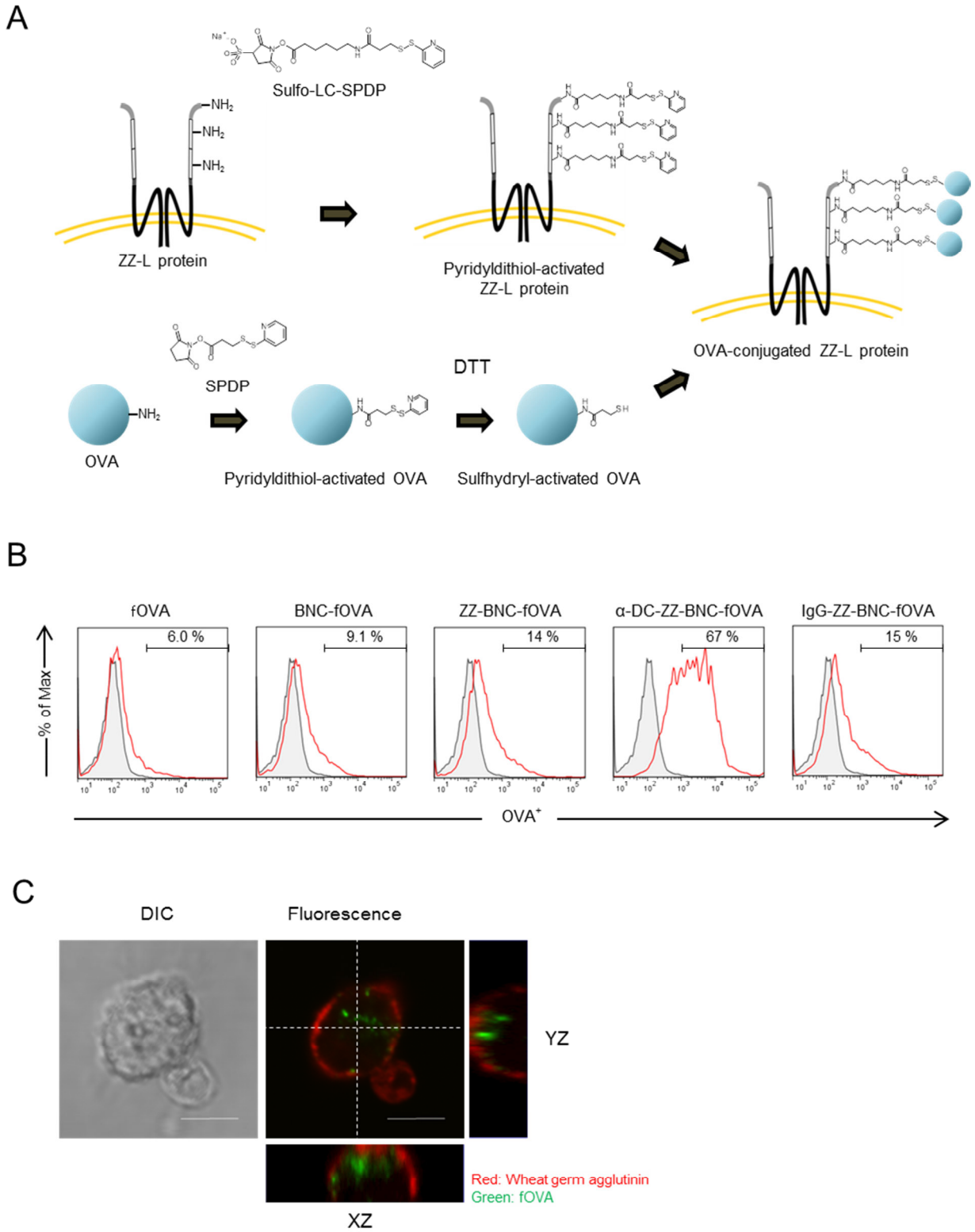

Fig. 3.2 Preparation of Ag-crosslinked α-DC-ZZ-BNC.
(A) Schematic representation of Ag-crosslinking to ZZ-BNC. (B) Isolated splenic DCs were incubated in the medium supplemented with each complex as same amount of OVA at 37 °C for 4 h, and then the cells were subjected to flow cytometric analysis. The values were indicated percentages of $fOVA^+$ cells in DCs. (C) The DC treated with α-DC-ZZ-BNC-fOVA was observed under a confocal laser scanning microscopy. Fluorescence derived from wheat germ agglutinin and fOVA is indicated in red and green, respectively. Scale bars, 5 μm.

3.4.2. In vivo DC-targeting through local injections

SC and IM routes are often used for vaccination at worldwide clinical sites, while IV route used for the targeting of splenic DCs with α-DC-ZZ-BNC [26] was scarcely utilized. In this study, I examined whether α-DC-ZZ-BNC could be used for the targeting DCs through SC and IM routes. When mice were administrated with CF750 (near-infrared fluorescent dye)-labeled α-DC-ZZ-BNC (10 μg as ZZ-L protein) through SC or IM routes and sacrificed after 12 h, each organ and LNs close to injection sites (tail base for SC, quadriceps femoris muscle for IM) were subjected to the observation under *in vivo* imaging system. Substantial amount of fluorescence was observed in LNs closest to injection sites (ILNs for SC, ILN and PLN for IM) and small amount of fluorescence in kidney (Fig. 3.3), while large amount of fluorescence was observed at injection sites and bladder. The accumulation of α-DC-ZZ-BNC complex in LNs strongly suggested that the complex was captured by APCs at either injection sites or LNs.

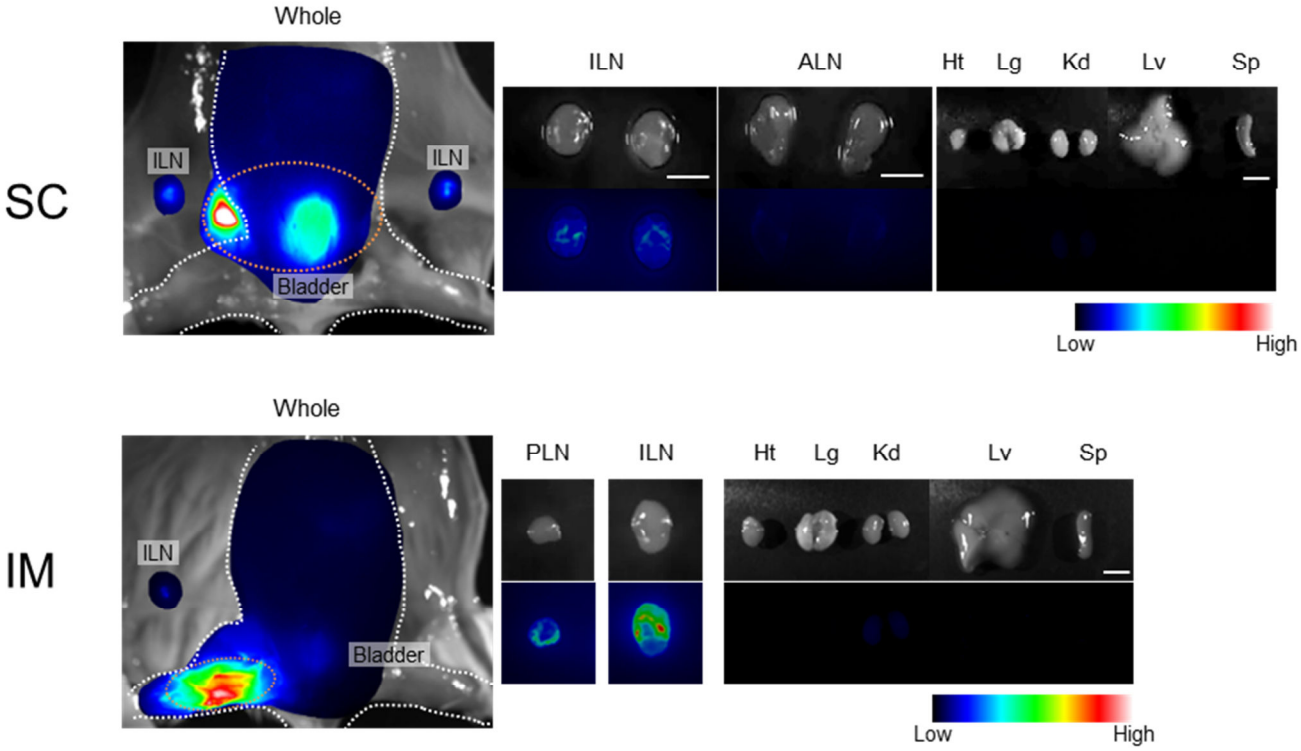

Fig. 3.3 *In vivo* distribution of α-DC-ZZ-BNC injected through SC and IM routes.
CF750-labeled α-DC-ZZ-BNC (10 μg as ZZ-L protein) was injected to mice through SC (upper) and IM (lower) routes. After 12 h, mice were sacrificed, and tissues (heart, Ht; lung, Lg; kidney, Kd; liver, Lv; spleen, Sp; LNs (inguinal, ILN; popliteal, PLN; axillary, ALN)) were isolated. Fluorescent signals in each tissues were observed by using *in vivo* imaging system. Scale bar in LN images, 3 mm; in organ images, 10 mm.

For deciphering target cells of α-DC-ZZ-BNC complex in each LN, mice were administrated with the complex SC or IM, and then sacrificed after 8, 12, and 24 h. The localization of CF633-labeled ZZ-BNC in the subsets of LNs ($CD11c^+$ cells, $CD11b^+$ cells, and $CD19^+$ cells) was analyzed by flow cytometer. As shown in Fig. 3.4A, α-DC-ZZ-BNC complex could target approximately 12% of $CD11c^+$ cells (*i.e.*, DCs) in ILNs more efficiently than ZZ-BNC (6%), IgG-ZZ-BNC, BNC, and 40-nm beads (< 1%, respectively) at 12 h after SC injection. The amount of α-DC-ZZ-BNC in the DCs reached maximal at 12 h, and then decreased at 24 h (Fig. 3.4B). When comparing with ZZ-BNC, the degree of DC targeting could be enhanced by α-CD11c IgGs to some extent. Moreover, α-DC-ZZ-BNC and ZZ-BNC could accumulate to $CD11b^+$ cells (including macrophages and myeloid DCs) after 8 h at comparable level (Fig. 3.4C), and $CD19^+$ cells (B cells) after 8 h to less extent (Fig. 3.4D). On the other hand, α-DC-ZZ-BNC complex injected IM could target approximately 9% of $CD11c^+$ cells in PLN at 12 h, which was higher than ZZ-BNC (5%), IgG-ZZ-BNC (< 1%), BNCs (1%), and 40-nm fluorescent beads (< 1%) (Fig. 3.5A). The α-DC-ZZ-BNC complex accumulated to the DCs at 8 h, earlier than the complex injected SC probably due to short distance from IM injection site to PLN, and then gradually decreased to 24 h (Fig. 3.5B). The degree of DC targeting of ZZ-BNC was lower than that of α-DC-ZZ-BNC. As for the accumulation of α-DC-ZZ-BNC and ZZ-BNC to $CD11b^+$ cells (*e.g.*, macrophages, myeloid DCs) and $CD19^+$ cells (B cells), any significant difference could not be found between SC and IM injections (Fig. 3.5C, D). The accumulation of these complexes to $CD11b^+$ cells might be caused by the interaction of high mannose-type sugar chains of ZZ-BNC with mannose receptors expressed abundantly on $CD11b^+$ cells [13]. The accumulation of these complexes to $CD19^+$ cells might be mediated by the interaction of ZZ domains with Ig molecules on $CD19^+$

cells [13]. These results strongly suggested that the α-DC-ZZ-BNC complex could efficiently target wide variety of APCs (*i.e.*, LN-resident DCs, migratory DCs, myeloid DCs, macrophages, and B cells) by the help of α-CD11c IgGs and ZZ-BNC components (ZZ domains, high mannose-type sugar chains; *see* above). Collectively, the α-DC-ZZ-BNC complex is suitable for delivering Ags to APCs for eliciting effective immunities.

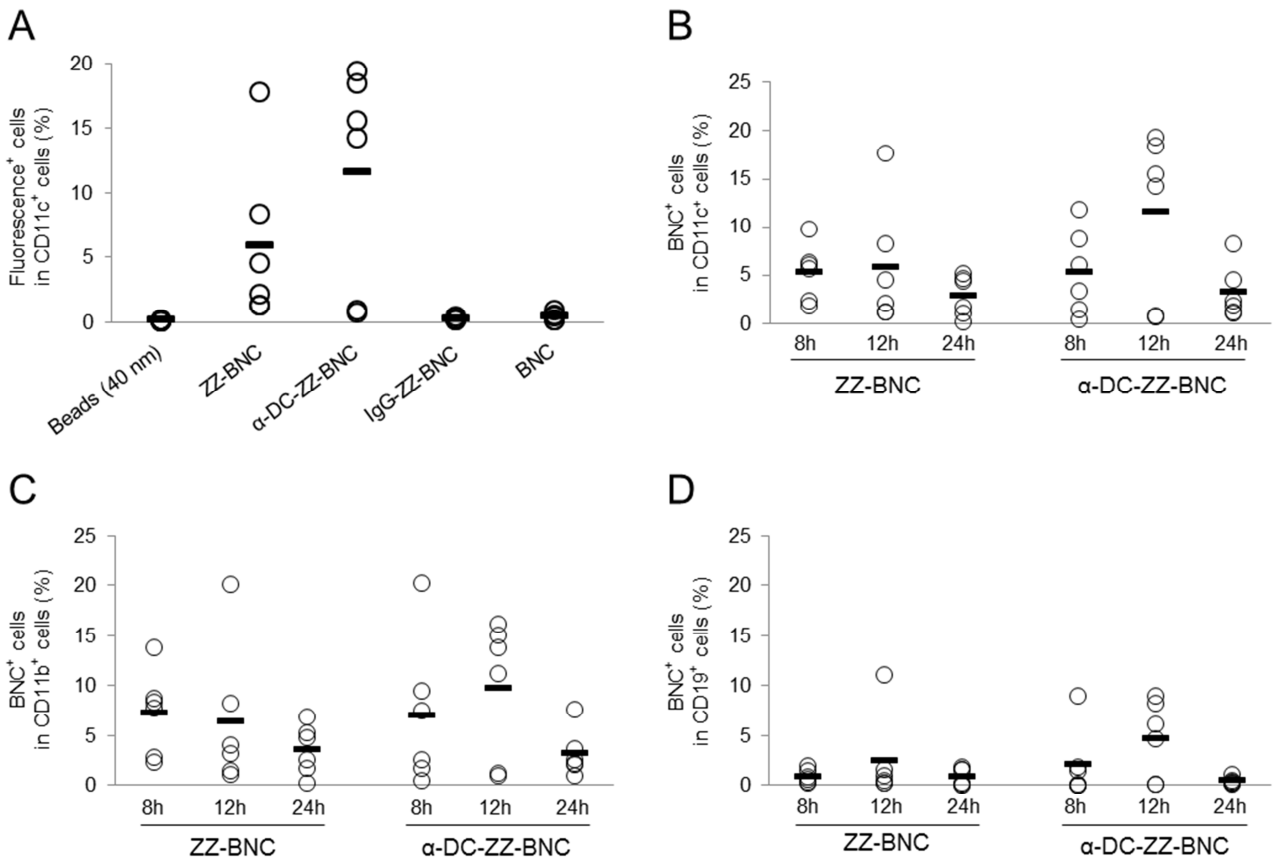

Fig. 3.4 *In vivo* accumulation of α-DC-ZZ-BNC injected through SC route to APCs in ILNs.
CF633-labeled α-DC-ZZ-BNC (10 μg as ZZ-L protein) was injected to mice through SC route. (A) After 12 h, mice were sacrificed, and ILN cells were isolated. The cells were stained with α-CD11c-FITC, and then subjected to flow cytometric analysis for evaluating the accumulation of each particle to DCs in ILN. At 8, 12, and 24 h after injection, accumulation of α-DC-ZZ-BNC to $CD11c^+$ cells (B), $CD11b^+$ cells (C), and $CD19^+$ cells (D) was analyzed. The percentages are indicated $fluorescence^+$ cells in each population. Measurements were performed with six mice in each group. Thick lines indicate average values from each group.

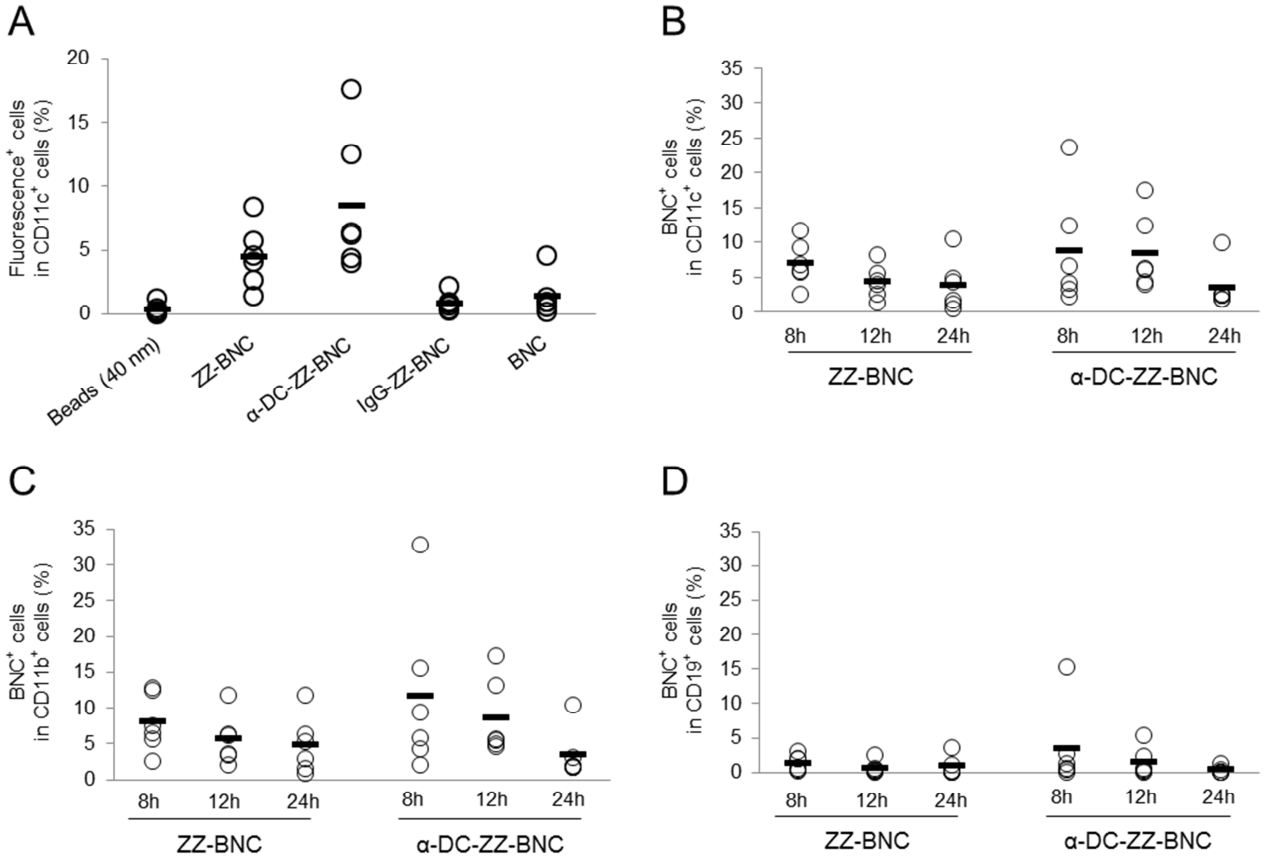

Fig. 3.5 *In vivo* accumulation of α-DC-ZZ-BNC injected through IM route to APCs in PLNs.
CF633-labeled α-DC-ZZ-BNC (10 μg as ZZ-L protein) was injected to mice through IM route. (A) After 12 h, mice were sacrificed, and PLN cells were isolated. The cells were stained with α-CD11c-FITC, and then subjected to flow cytometric analysis for evaluating the accumulation of each particle to DCs in PLN. At 8, 12, and 24 h after injection, accumulation of α-DC-ZZ-BNC to $CD11c^+$ cells (B), $CD11b^+$ cells (C), and $CD19^+$ cells (D) was analyzed. The percentages are indicated $fluorescence^+$ cells in each population. Measurements were performed with six mice in each group. Thick lines indicate average value from each group.

3.4.3. Induction of DC maturation with α-DC-ZZ-BNC-OVA

Co-stimulatory molecules on DCs, such as CD80 and CD86, play an important role in DC maturation, followed by Ag-presentation for providing stimulatory signals to naïve T cells. CD40 (tumor necrosis factor receptor) mediates subsequent DC maturation by interaction with CD40 ligands [14]. In this study, I examined if the α-DC-ZZ-BNC-OVA complex could elicit DC maturation without any adjuvant. Isolated splenic DCs were incubated in the medium containing α-DC-ZZ-BNC-OVA at 37 °C for 24 h, and then the expression levels of CD80, CD86, and CD40 were analyzed by using flow cytometer. Based on the mean fluorescent intensity, the expression level of CD80 was elevated with ZZ-BNC-OVA and α-DC-ZZ-BNC-OVA by 1.9-fold and 2.2-fold (OVA alone as control), respectively (Fig. 3.6A). The expression levels of CD86 and CD40 were also elevated with ZZ-BNC-OVA and α-DC-ZZ-BNC-OVA to similar extent (Fig. 3.6B, C). It was therefore revealed that both α-DC-ZZ-BNC-OVA and ZZ-BNC-OVA could elicit effective *ex vivo* DC maturation without any adjuvant. Because of low signal-to-noise ratio caused by the lack of SPF (specific pathogen-free) animal facility in our laboratory, I could not examine the *in vivo* DC maturation for differentiating α-DC-ZZ-BNC-OVA from ZZ-BNC-OVA. It has been still controversial whether α-CD11c IgG moiety of α-DC-ZZ-BNC-OVA contributes to the enhancement of *in vivo* DC maturation or not.

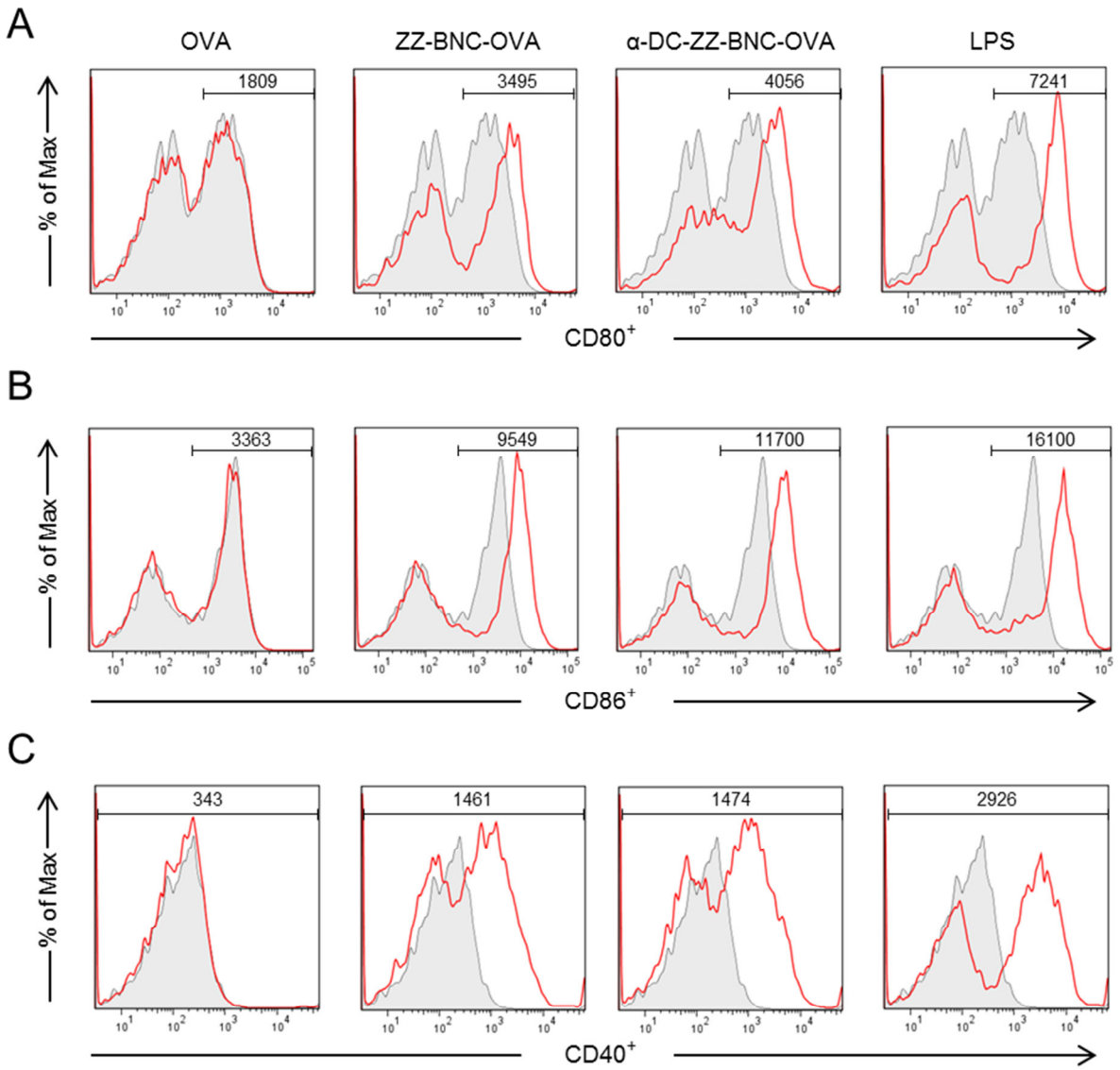

Fig. 3.6 Induction of DC maturation with α-DC-ZZ-BNC-OVA.
Splenic DCs were incubated in the medium supplemented with OVA, ZZ-BNC-OVA, α-DC-ZZ-BNC-OVA as a same amount of OVA. As positive control, LPS was added to the culture. After 24 h, the cells were stained with APC-labeled α-CD80 IgG (A), α-CD86 IgG (B), andα-CD40 IgG (C), and then subjected to flow cytometric analysis. The values were indicated mean fluorescent intensity of the each gated DC.

3.4.4. Induction of OVA-specific CTL proliferation with α-DC-ZZ-BNC-OVA

Both Ag-specific T cell responses and IgG subtypes were analyzed by using OVA as a model Ag. Splenocytes were isolated from OVA-immunized mice (7 days after immunization), treated with H-2k^b OVA tetramer-SIINFEKL (fluorescence-labeled tetramer of the complex of MHC molecule and epitope of OVA-specific CTL-derived T cell receptor) and α-CD8-FITC, and then subjected to flow cytometer to detect OVA-specific CD8$^+$ T cells (Fig. 3.7A). Comparing with OVA alone, the ZZ-BNC-OVA and α-DC-ZZ-BNC-OVA could enhance the proliferation of OVA-specific CD8$^+$ T lymphocytes moderately and efficiently, respectively (Fig. 3.7B). Even if Ag is less immunogenic, α-DC-ZZ-BNC could enhance Ag-specific cellular immunity by inducing proliferation of CTL.

3.4.5. Evaluation of Th1- and Th2-related immune responses induced with α-DC-ZZ-BNC-OVA

IFN-γ secretion is a marker of Th1-related immune responses. Splenocytes isolated from the mice immunized with α-DC-ZZ-BNC-OVA (7 days after last immunization) were cultured in the presence of OVA for 7 days, and the culture medium was subjected to the ELISA for IFN-γ. As shown in Fig. 3.7C, α-DC-ZZ-BNC-OVA and ZZ-BNC-OVA were found to induce IFN-γ secretion at 448 and 224 pg/ml, respectively, while OVA itself could not. Taken together, even if Ag is less immunogenic, α-DC-ZZ-BNC and ZZ-BNC could induce the proliferation of Ag-specific Th1 cells in accompany with IFN-γ secretion. Especially, DC-targeting driven by α-CD11c IgG was effective for this enhancement.

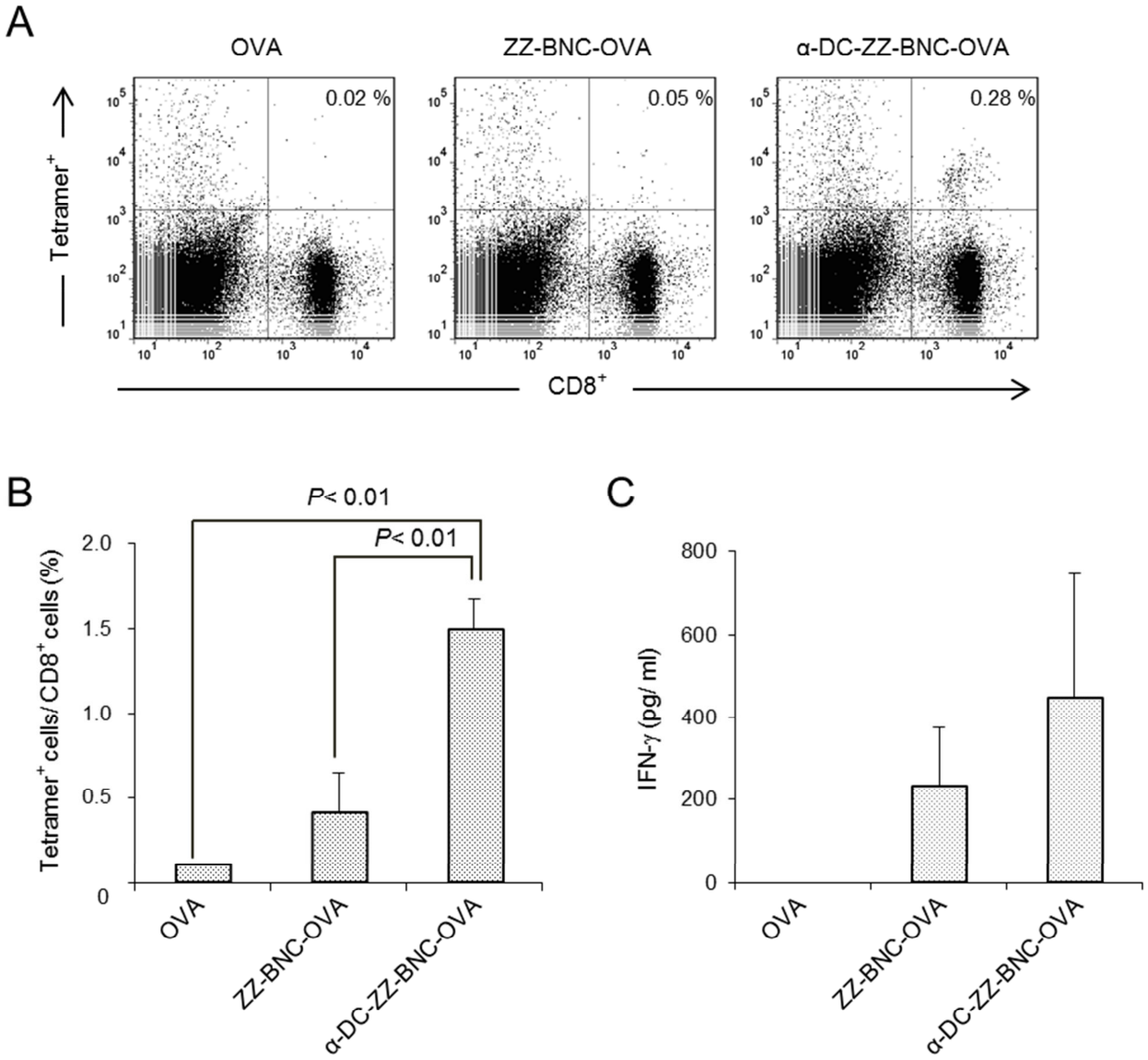

Fig. 3.7 Proliferation of OVA-specific CTL and Th cells induced by immunization with α-DC-ZZ-BNC-OVA.

(A) After 7 days from SC injection of α-DC-ZZ-BNC-OVA (10 μg as OVA), C57BL/6 mice were sacrificed, and the splenocytes were isolated. The cells were stained with APC-labeled H-2k^b OVA tetramer and FITC-labeled α-CD8 IgG for detection of OVA-specific CD8$^+$ T lymphocytes with flow cytometer. The values in figure indicate percentages of OVA-specific CD8$^+$ T lymphocytes in splenocytes. (B) Statistic analysis of the CTL proliferation was indicated. Measurements were performed in triplicate. Error bars indicate the SEM. (C) The splenocytes were incubated the medium supplemented with OVA at 37 °C for 7 days. The IFN-γ concentrations of supernatants were quantified by using ELISA. Measurements were performed in triplicate. Error bars indicate the SEM.

IFN-γ and IL-4 are secreted from Th1 and Th2, contributing to Ig class-switch from IgM to IgG2a and IgG1 in B cells, respectively [32]. Mice were immunized with various forms of OVA three times at 0, 2, and 4 weeks, sera were collected from the mice at 5 weeks, and then subjected to ELISA for α-OVA IgG1 and IgG2a. The OVA vaccines used were as follows: α-DC-ZZ-BNC-OVA, ZZ-BNC-OVA (α-DC IgG-less control), IgG-ZZ-BNC-OVA (no targeting control), α-CD11c-OVA (BNC-less control), and OVA with Alum (OVA/Alum, positive control for Th2-dependent immunity [12]). As for the Th2-dependent immunity, all BNC-containing vaccines showed strong induction of α-OVA IgG1, comparable to OVA/Alum (Fig. 3.8A). The α-CD11c-OVA induced slightly low level of α-OVA IgG1. As for the Th1-dependent immunity, while OVA/Alum and α-CD11c-OVA were less immunogenic, all BNC-containing vaccines showed about 100-fold higher level of α-OVA IgG2a induction than other vaccines (Fig. 3.8B). These results suggested that BNC-containing vaccines could induce Th1 and Th2 immunities effectively. However, there was no significant difference among BNC-containing vaccines, indicating that α-CD11c IgG is not necessary for the production of IgGs. The ZZ-BNC components (ZZ domains, high mannose-type sugar chains) and clustered Ags may contribute to the production of IgGs through sufficient DC maturation, because α-CD11c-OVA was less immunogenic presumably by insufficient DC maturation due to the lack of these functional domains.

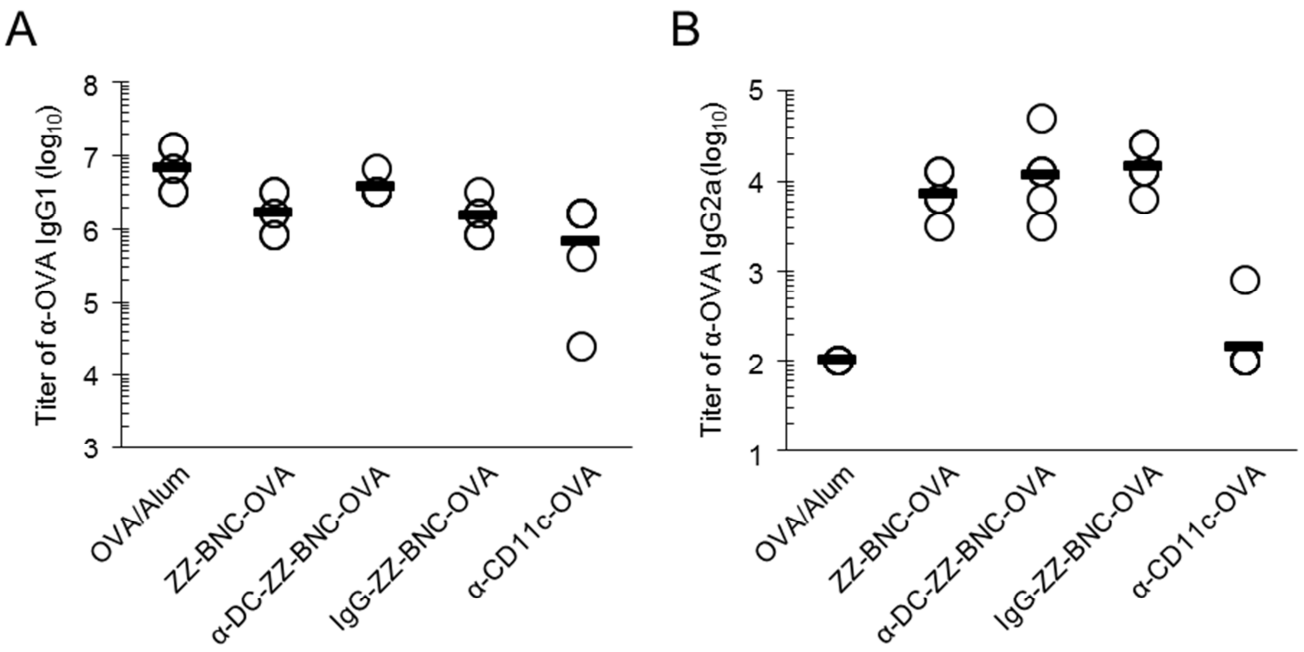

Fig. 3.8 Induction of OVA-specific IgGs production with α-DC-ZZ-BNC-OVA.
Mice were received SC injection of α-DC-ZZ-BNC-OVA (10 μg as OVA) at week 0, 2, and 4. Sera were collected from the immunized mice, and then titers of OVA-specific IgG1 (A) and IgG2a (B) in sera were determined by using ELISA. Measurements were performed with six mice in each group. Thick lines indicate average titers from each group.

3.4.6. Protective immunity induced with α-DC-ZZ-BNC-based vaccine

In the previous study, ZZ-BNC conjugated with JEV-derived D3 (ZZ-BNC-D3) was demonstrated to show good immunogenicity and sufficient protective efficacy against JEV challenge [27]. It was therefore considered that ZZ-BNC could not only improve immunogenicity of D3 by clustering onto ZZ-BNC but also deliver D3 to APCs by ZZ-BNC components (ZZ domains, high mannose-type sugar chains). In this study, I evaluate the effect of DC targeting by α-CD11c IgG on the protective efficacy against JEV challenge. According to the preparation protocol for α-DC-ZZ-BNC-OVA, bacterially expressed JEV-derived D3 was conjugated with α-DC-ZZ-BNC to form α-DC-ZZ-BNC-D3. The particle properties of the complex were similar to those of α-DC-ZZ-BNC-OVA (Table 3.3). Mice were immunized with α-DC-ZZ-BNC-D3 through SC injection 3 times with 2 weeks interval (0, 2, 4 weeks), and sera were collected after 2 weeks from last injection (6 weeks). As control vaccines, α-CD11c-D3 (BNC-less control), ZZ-BNC-D3 (α-CD11c IgG-less control), and D3 alone were used for evaluating the effect of each component of α-DC-ZZ-BNC-D3 on the immunogenicity of D3. As shown in Fig. 3.9A, α-DC-ZZ-BNC-D3 could induce α-JEV total IgG production more efficiently than D3 alone, but there were no significant difference among α-DC-ZZ-BNC-D3, ZZ-BNC-D3, and α-CD11c-D3. When α-JEV IgG1 and IgG2a were measured by ELISA, both α-DC-ZZ-BNC-D3 and ZZ-BNC-D3 could enhance IgG1 and IgG2a production more efficiently than α-CD11c-D3 and D3 alone (Fig. 3.9B), suggesting that BNC-containing vaccines could induce Th1 and Th2 immunities effectively regardless of the presence of α-CD11c IgG. As demonstrated in the BNC-containing OVA vaccines (see above), it was corroborated that the ZZ-BNC components (ZZ domains, high mannose-type sugar chains) and clustered Ags might

contribute to the production of IgGs through sufficient DC maturation.

Table 3.3 Particle properties of α-DC-ZZ-BNC-D3 analyzed by a DLS.

Samples	Z-average (nm)	PDI	ζ-potential (mV)
ZZ-BNC-D3	70.2 ± 10	0.324 ± 0.06	-23.7 ± 7.0
α-DC-ZZ-BNC-D3	74.6 ± 14	0.341 ± 0.11	-24.3 ± 7.2

Measurements were performed in triplicate. Values are indicated as mean ± SD.

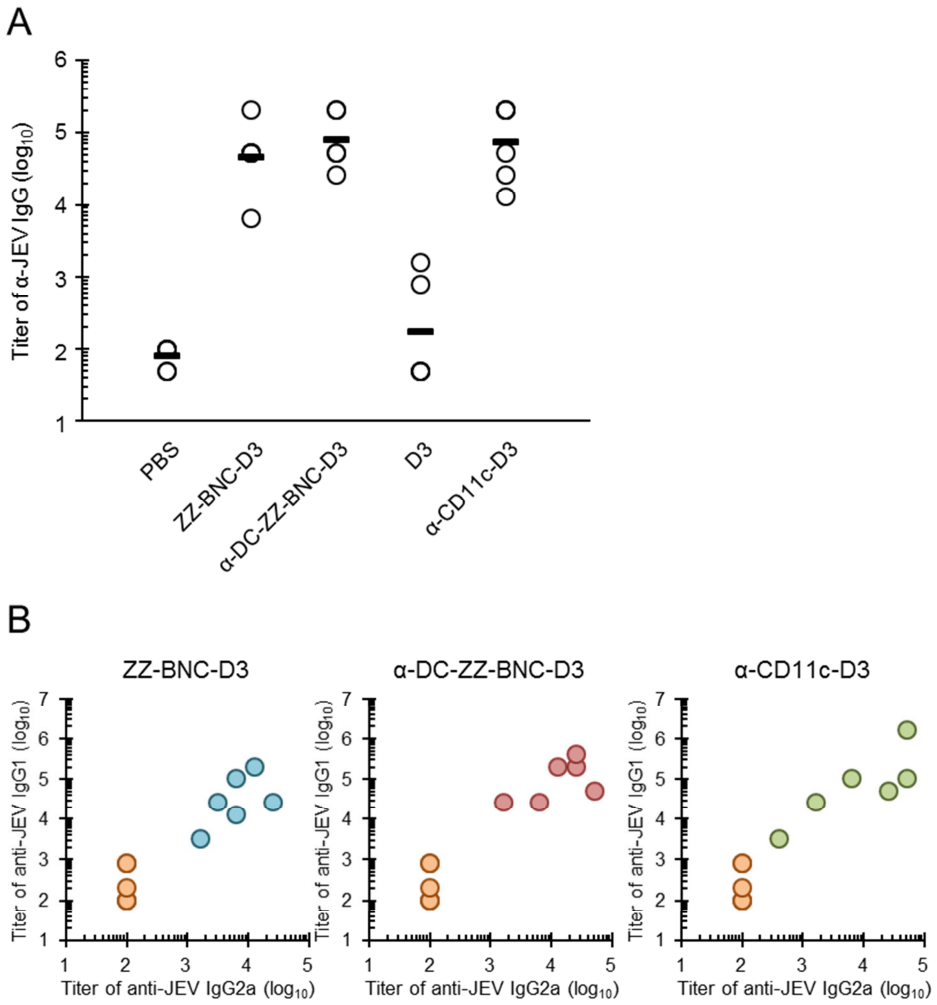

Fig. 3.9 Induction of JEV-specific IgGs production with α-DC-ZZ-BNC-D3.

Mice were received SC injection of α-DC-ZZ-BNC-D3 (30 μg as D3) at week 0, 2, and 4. Sera were collected from the immunized mice, and then titers of JEV-specific total IgG (A), IgG1, and IgG2a (B) in sera were determined by using ELISA. Titers of IgG1/IgG2a in sera from mice immunized with D3 alone, ZZ-BNC-D3, α-DC-ZZ-BNC-D3, and α-CD11c-D3 are indicated in orange, blue, red, and green, respectively. Measurements were performed with six mice in each group. Thick lines indicate average titers from each group.

At 2 weeks from last injection (6 weeks), immunized mice were inoculated with 50-times dose of LD_{50} of the JEV JaGAr01 strain intraperitoneally, and then survival rates were recorded for 20 days (Fig. 3.10). Immunization with α-DC-ZZ-BNC-D3 could protect 80% of the immunized mice from JEV challenge, while survival rates of the mice immunized with ZZ-BNC-D3, α-CD11c-D3, and D3 alone were 50%, 33%, and 17%, respectively. Thus, α-DC-ZZ-BNC-D3 could induce most effective protective immunity among vaccines used. Although the titers of α-JEV IgGs elicited by α-DC-ZZ-BNC-D3, ZZ-BNC-D3, and α-CD11c-D3 were comparable (see Fig. 3.9), the DC targeting driven by α-CD11c IgG successfully contributed to the survival of JEV-challenged mice. This result suggested that the DC targeting could enhance cellular immunity rather than humoral immunity. Additionally, it has been known that CTL plays a pivotal role in the protection against West Nile virus infection, belonging to the same family of JEV [33-35].

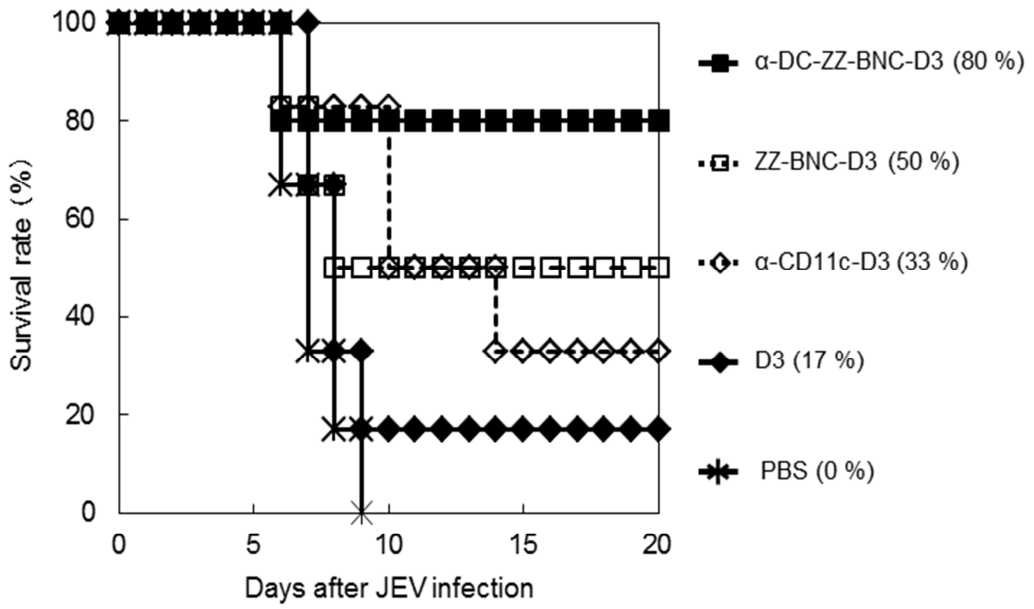

Fig. 3.10 Survival of the mice immunized with α-DC-ZZ-BNC-D3 against JEV challenge.
The mice immunized with α-DC-ZZ-BNC-D3 were challenged intraperitoneally with 50-times dose of 50% lethal dose ($50LD_{50}$) of the JEV JaGAr01 strain followed by intracerebral inoculation with PBS. The mice were subjected to monitoring the signs of illness/distress such as ruffled fur or paralysis and recording the survival rates.

3.5. Discussion

DC-specific Ag delivery has been considered as a promising strategy for facilitating efficient recognition, processing, and presentation of Ags by DCs, leading to enhance the Ag-specific immunity. Generally, for elicitation of adaptive immunities, vaccines should induce effective innate immunity by providing stimulatory signals to APC via PRRs (including Toll-like receptors) [11]. Adjuvants can elicit innate immunity by interacting with PRRs to stimulate the secretion of cytokines [12]. However, either non-specific or over elicitation of innate immunity by adjuvants should be avoided for the guarantee of their safety, because wide variety of host cells harbors PRRs. These situations have led me to deliver adjuvants in a DC-specific manner by using DC-targeting nanocarriers. In Chapter II, it was revealed that α-DC-ZZ-BNC could accumulate into splenic DCs through IV injection and the α-DC-ZZ-BNC-LP-Ag complex could elicit Ag-specific IgG production efficiently [26]. Contrary, the complex could not elicit sufficient immunological responses through local injections (SC), which have been used at worldwide clinical sites (Fig. 3.1), presumably due to the *in vivo* non-specific bindings caused by its positive charge. For optimizing the particle properties (*e.g.*, charge, size) of α-DC-ZZ-BNC-based vaccines, the Ag incorporation method was changed from LP fusion to chemical crosslinking. When fOVA was used as model Ag, the α-DC-ZZ-BNC-fOVA could deliver fOVA into DCs *ex vivo* more efficiently rather than fOVA alone, ZZ-BNC-fOVA, and IgG-ZZ-BNC-fOVA. Importantly, the fOVA delivered with α-DC-ZZ-BNC-fOVA was localized at the intracellular fraction of DCs (Fig. 3.2B, C). CD11c molecule forms heterodimeric CR4 with CD18 molecule, involved in the incorporation of pathogens by DCs [36]. Cellular uptake of fOVA by CR4 might be enhanced by targeting CD11c molecules with α-DC-ZZ-BNC. These results suggested

that anionic LPs are more suitable for the *in vivo* DC-specific Ag delivery using α-DC-ZZ-BNC-LP-Ag rather than cationic LPs.

Followed by the formulation of α-DC-ZZ-BNC, the complex was administrated via local injections (SC and IM). *In vivo* imaging analysis indicated the accumulation of α-DC-ZZ-BNC to the LNs closest to the injection sites (Fig. 3.3). Flow cytometric analysis demonstrated that α-DC-ZZ-BNC injected either SC or IM accumulated to approximately 10% of DCs in the LNs, of which the efficiency was higher than 40-nm beads and ZZ-BNC (Figs. 3.4A, 3.5A). Interestingly, both α-DC-ZZ-BNC and ZZ-BNC could accumulate not only to DCs but also to $CD11b^+$ cells (*e.g.*, macrophages and myeloid DCs) and $CD19^+$ cells (B cells), corroborating the pleiotropic APC-targeting function of ZZ-BNC is sustained by the interactions of its components with APC surface receptors (*i.e.*, the interaction of ZZ domains and high mannose-type sugar chains with Ig molecules and C-type lectin receptors (CLR), respectively). Moreover, α-DC-ZZ-BNC is the most effective APC-targeting nanocarrier driven by synergistic action of α-CD11c IgGs and ZZ-BNC components.

Concerning about the contribution of α-CD11c IgG to the immunological responses elicited by α-DC-ZZ-BNC-Ag, although significant contributions were observed in Ag-dependent CTL proliferation (Fig. 3.7B), Th1 cytokine secretion (Fig. 3.7C), and induction of protective immunity (Fig. 3.10), no contribution was observed in induction of *ex vivo* DC maturation (Fig. 3.6), Ag-dependent IgG production (Fig. 3.8), and induction of IgG class switch (Fig. 3.8). These results demonstrated that α-DC-ZZ-BNC-Ag rather than ZZ-BNC-Ag could elicit T cell-dependent immune responses effectively. Taking the advantage of α-CD11c IgG in *in vivo* DC targeting into considerations, α-DC-ZZ-BNC-Ag could presumably induce *in vivo* DC maturation more robustly than ZZ-BNC-Ag. Since the incorporation of Ag with

α-CD11c IgG could induce effective DC maturation through the interaction with CR4 in a Toll-like receptor-independent manner [37], the α-CD11c IgG moiety of α-DC-ZZ-BNC-Ag could also induce *in vivo* DC maturation, followed by the induction of subsequent humoral and cellular immunities. On the other hand, efficient translocation of Ags from endosome to cytoplasm is indispensable for the induction of Ag-dependent CTL proliferation [13, 14]. It was speculated that the α-CD11c IgG could enhance the endosomal escape of Ags through the interaction of α-DC-ZZ-BNC-Ag with CR4 by the help of HBV-derived membrane fusogenic activity of ZZ-BNC.

As discussed previously, ZZ-BNC harbors three important functions for inducing immunological responses (*i.e.*, ZZ domains, high mannose-type sugar chains, Ag clustering). Comparing with Ag alone, ZZ-BNC-Ag showed advantages in the following issues: *ex vivo* DC maturation (Fig. 3.6), Ag-dependent CTL proliferation (Fig. 3.7B), Th1 cytokine secretion (Fig. 3.7C), Ag-dependent IgG production (Fig. 3.8), induction of IgG class switch (Fig. 3.8), and induction of protective immunity (Fig. 3.10). It was demonstrated that ZZ-BNC by itself functions as an APC-specific DDS nanocarrier. ZZ domains might interact with Ig molecules on B cells, leading to Ag presentation [38]. High mannose-type sugar chains might interact with CLRs (*e.g.*, DC-SIGN, DNGR-1), eliciting innate immunity [39]. Especially, while α-DC-ZZ-BNC is the most potent APC-specific DDS nanocarrier in this study, α-CD11c IgG is operative only in mice. The ZZ-BNC is a more versatile DDS nanocarrier for wide variety of animals than α-DC-ZZ-BNC.

Comparing α-CD11c-D3 with ZZ-BNC-D3, the protective immunity against JEV challenge was more successful for ZZ-BNC-D3 (Fig. 3.10), while there was little difference in D3-dependent IgG productions (total IgG, IgG1, IgG2a) (Fig. 3.9). It was

therefore postulated that ZZ-BNC-D3 could induce D3-specific CTL proliferation more effectively than α-CD11c-D3. When OVA was used instead of D3, both vaccines could induce sufficient α-OVA IgG1 without any adjuvant, which is comparable level of OVA with Alum (Fig 3.8A). Meanwhile, α-CD11c-OVA could induce less α-OVA IgG2a than ZZ-BNC-OVA (Fig. 3.8B). Collectively, as described above, the ZZ-BNC components would stimulate PRRs and consequently induce robust Th1 and Th2 immunities. Since α-CD11c-OVA lacks HBV-derived membrane fusogenic activity, the endosomal escape of OVA, indispensable for OVA-specific CTL proliferation, may be less efficient in α-CD11c-OVA rather than in ZZ-BNC-OVA.

Taken together, both α-DC-ZZ-BNC-Ag and ZZ-BNC-Ag are revealed as a promising APC-targeting nanocarrier for forthcoming vaccines. They could induce effective DC maturation, leading to the induction of humoral and cellular immunities to sufficient levels for protecting viral infections. Further studies on the regulation of intracellular trafficking of this nanocarrier are necessary for optimizing the ratio of humoral immunity to cellular immunity of APC-targeting BNC-based vaccines, which is indispensable for developing best vaccine against each pathogen.

3.6. Conclusion

The α-DC-ZZ-BNC could target DCs *in vivo* through local injections as well as systemic injection. The α-DC-ZZ-BNC-Ag complex could deliver Ags to the intracellular fraction of DCs efficiently, followed by induction of DC maturation, proliferation of Ag-specific CTL and Th cells, and Ag-specific IgG production. These immunological responses could confer sufficient protective immunities against virus infection in mice, demonstrating that the DC-specific Ag delivery with α-DC-ZZ-BNC is a promising platform for forthcoming vaccines.

3.7. References

1. C.L. van Broekhoven, C.R. Parish, C. Demangel, W.J. Britton, J.G. Altin, Targeting dendritic cells with antigen-containing liposomes: a highly effective procedure for induction of antitumor immunity and for tumor immunotherapy, Cancer Res. 64 (2004) 4357–4365.
2. J.S. Lewis, T.D. Zaveri, C.P. Crooks, B.G. Keselowsky, Microparticle surface modifications targeting dendritic cells for non-activating applications, Biomaterials 33 (2012) 7221–7232.
3. R.W. Carter, C. Thompson, D.M. Reid, S.Y.C. Wong, D.F. Tough, Preferential induction of $CD4^+$ T cell responses through *in vivo* targeting of antigen to dendritic cell-associated C-type lectin-1, J. Immunol. 177 (2006) 2276–2284.
4. S. Hamdy, A. Haddadi, A. Shayeganpour, J. Samuel, A. Lavasanifar, Activation of antigen-specific T cell-responses by mannan-decorated PLGA nanoparticles, Pharm. Res. 28 (2011) 2288–2301.
5. K.C. Sheng, M. Kalkanidis, D.S. Pouniotis, S. Esparon, C.K. Tang, V. Apostolopoulos, G.A. Pietersz, Delivery of antigen using a novel mannosylated dendrimer potentiates immunogenicity *in vitro* and *in vivo*, Eur. J. Immunol. 38 (2008) 424–436.
6. Y.J. Kwon, E. James, N. Shastri, J.M.J. Fréchet, *In vivo* targeting of dendritic cells for activation of cellular immunity using vaccine carriers based on pH-responsive microparticles, Proc. Natl. Acad. Sci. U.S.A. 102 (2005) 18264–18268.
7. K. Serre, P. Machy, J.C. Grivel, G. Jolly, N. Brun, J. Barbet, L. Leserman, Efficient presentation of multivalent antigens targeted to various cell surface

molecules of dendritic cells and surface Ig of antigen-specific B cells, J. Immunol. 161 (1998) 6059-6067.

8. K. Serre, L. Giraudo, L. Leserman, P. Machy, Liposomes targeted to Fc receptors for antigen presentation by dendritic cells *in vitro* and *in vivo*, Methods Enzymol. 373 (2003) 100–118.

9. L.J. Cruz, P.J. Tacken, F. Rueda, J.C. Domingo, F. Albericio, C.G. Figdor, Targeting nanoparticles to dendritic cells for immunotherapy, Methods Enzymol. 509 (2012) 143-163.

10. J.P. Amorij, G.F.A. Kersten, V. Saluja, W.F. Tonnis, W.L.J. Hinrichs, B. Slütter, S.M. Bal, J.A. Bouwstra, A. Huckriede, W. Jiskoot, Towards tailored vaccine delivery: needs, challenges and perspectives, J. Control. Release 161 (2012) 363–376.

11. A. Iwasaki, R. Medzhitov, Regulation of adaptive immunity by the innate immune system, Science 327 (2010) 291–295.

12. S. Awate, L.A. Babiuk, G. Mutwiri, Mechanisms of action of adjuvants, Front. Immunol. 4 (2013) 114-123.

13. E.S. Trombetta, I. Mellman, Cell biology of antigen processing *in vitro* and *in vivo*, Annu. Rev. Immunol. 23 (2005) 975–1028.

14. J. Banchereau, F. Briere, C. Caux, J. Davoust, S. Lebecque, Y. Liu, B. Pulendran, K. Palucka, Immunobiogy of dendritic cells, Immunology 18 (2000) 767–811.

15. E. Yuba, Y. Kono, A. Harada, S. Yokoyama, M. Arai, K. Kubo, K. Kono, The application of pH-sensitive polymer-lipids to antigen delivery for cancer immunotherapy, Biomaterials 34 (2013) 5711–5721.

16. J.W. Yewdell, Designing $CD8^+$ T cell vaccines: it's not rocket science (yet).,

Curr. Opin. Immunol. 22 (2010) 402–410.

17. M.F. Bachmann, G.T. Jennings, Vaccine delivery: a matter of size, geometry, kinetics and molecular patterns, Nat. Rev. Immunol. 10 (2010) 787–796.

18. T. Yamada, H. Iwabuki, T. Kanno, H. Tanaka, T. Kawai, H. Fukuda, A. Kondo, M. Seno, K. Tanizawa, S. Kuroda, Physicochemical and immunological characterization of hepatitis B virus envelope particles exclusively consisting of the entire L (pre-S1 + pre-S2 + S) protein, Vaccine 19 (2001) 3154–3163.

19. S. Kuroda, S. Otaka, T. Miyazaki, M. Nakao, Y. Fujisawa, Hepatitis B virus envelope L protein particles. Synthesis and assembly in *Saccharomyces cerevisiae*, purification and characterization, J. Biol. Chem. 267 (1992) 1953–1961.

20. T. Yamada, Y. Iwasaki, H. Tada, H. Iwabuki, M.K.L. Chuah, T. VandenDriessche, H.Fukuda, A. Kondo, M. Ueda, M. Seno, K. Tanizawa, S. Kuroda, Nanoparticles for the delivery of genes and drugs to human hepatocytes, Nat. Biotechnol. 21 (2003) 885–890.

21. M. Yamada, A. Oeda, J. Jung, M. Iijima, N. Yoshimoto, T. Niimi, S.Y. Jeong, E.K. Choi, K. Tanizawa, S. Kuroda, Hepatitis B virus envelope L protein-derived bio-nanocapsules: Mechanisms of cellular attachment and entry into human hepatic cells, J. Control. Release 160 (2011) 322-329.

22. J. Jung, T. Matsuzaki, K. Tatematsu, T. Okajima, K. Tanizawa, S. Kuroda, Bio-nanocapsule conjugated with liposomes for *in vivo* pinpoint delivery of various materials., J. Control. Release 126 (2008) 255–264.

23. N. Kurata, T. Shishido, M. Muraoka, T. Tanaka, C. Ogino, H. Fukuda, A. Kondo, Specific protein delivery to target cells by antibody-displaying

bionanocapsules, J. Biochem. 144 (2008) 701–707.

24. M. Iijima, H. Kadoya, S. Hatahira, S. Hiramatsu, G. Jung, A. Martin, J. Quinn, J. Jung, S.Y. Jeong, E.K. Choi, T. Arakawa, F. Hinako, M. Kusunoki, N. Yoshimoto, T. Niimi, K. Tanizawa, S. Kuroda, Nanocapsules incorporating IgG Fc-binding domain derived from *Staphylococcus aureus* protein A for displaying IgGs on immunosensor chips, Biomaterials 32 (2011) 1455–1464.

25. Y. Tsutsui, K. Tomizawa, M. Nagita, H. Michiue, T. Nishiki, I. Ohmori, M. Seno, H. Matsui, Development of bionanocapsules targeting brain tumors, J. Control. Release 122 (2007) 159–164.

26. H. Matsuo, N. Yoshimoto, M. Iijima, T. Niimi, J. Jung, S.Y. Jeong, E.K. Choi, T. Sewaki, T. Arakawa, S. Kuroda, Engineered hepatitis B virus surface antigen L protein particles for *in vivo* active targeting of splenic dendritic cells, Int. J. Nanomedicine 7 (2012) 3341–3350.

27. T. Miyata, S. Tafuku, T. Harakuni, M. Tadano, N. Yoshimoto, M. Iijima, H. Matsuo, G. Matsuzaki, S. Kuroda, T. Arakawa, A bio-nanocapsule containing envelope protein domain III of Japanese encephalitis virus protects mice against lethal Japanese encephalitis virus infection, Microbiol. Immunol. 57 (2013) 470–477.

28. M. Iijima, T. Matsuzaki, H. Kadoya, S. Hatahira, S. Hiramatsu, G. Jung, K. Tanizawa, S. Kuroda, Bionanocapsule-based enzyme-antibody conjugates for enzyme-linked immunosorbent assay, Anal. Biochem. 396 (2010) 257–261.

29. M. Iijima, T. Matsuzaki, N. Yoshimoto, T. Niimi, K. Tanizawa, S. Kuroda, Fluorophore-labeled nanocapsules displaying IgG Fc-binding domains for

the simultaneous detection of multiple antigens, Biomaterials 32 (2011) 9011–9020.

30. S. Tafuku, T. Miyata, M. Tadano, R. Mitsumata, H. Kawakami, T. Harakuni, T. Sewaki, T. Arakawa, Japanese encephalitis virus structural and nonstructural proteins expressed in *Escherichia coli* induce protective immunity in mice, Microbes Infect. (2011) 4–11.

31. S.M. Moghimi, A.C. Hunter, J.C. Murray, Long-circulating and target-specific nanoparticles: theory to practice, Pharmacol. Rev. 53 (2001) 283–318.

32. S.L. Swain, K.K. McKinstry, T.M. Strutt, Expanding roles for $CD4^+$ T cells in immunity to viruses, Nat. Rev. Immunol. 12 (2012) 136–148.

33. B. Shrestha, M.S. Diamond, Role of $CD8^+$ T cells in control of West Nile Virus infection, J. Virol. 78 (2004) 8312-8321.

34. B. Shrestha, M.A. Samuel, M.S. Diamond, $CD8^+$ T cells require perforin to clear West Nile virus from infected neurons, J. Virol. 80 (2006) 119-129.

35. Y. Wang, M. Lobigs, E. Lee, A. Müllbacher, $CD8^+$ T cells mediate recovery and immunopathology in West Nile virus encephalitis, J. Virol. 77 (2003) 13323-13334.

36. G.D. Keizer, A.A. Te Velde, R. Schwarting, C.G. Figdor, J.E. De Vries, Role of p150,95 in adhesion, migration, chemotaxis and phagocytosis of human monocytes, Eur. J. Immunol. 17 (1987) 1317–1322.

37. A.L. White, A.L. Tutt, S. James, K.A. Wilkinson, F.V. Castro, S.V. Dixon, J. Hitchcock, M. Khan, A. Al-Shamkhani, A.F. Cunningham, M.J. Glennie, Ligation of CD11c during vaccination promotes germinal centre induction and robust humoral responses without adjuvant, Immunology 131 (2010)

141–151.

38. M.R. Clark, D. Massenburg, K. Siemasko, P. Hou, M. Zhang, B-cell antigen receptor signaling requirements for targeting antigen to the MHC class II presentation pathway, Curr. Opin. Immunol. 16 (2004) 382–387.

39. M.J. Robinson, D. Sancho, E.C. Slack, S. LeibundGut-Landmann, C. Reis e Sousa, Myeloid C-type lectins in innate immunity, Nat. Immunol. 7 (2006) 1258–1265.

Chapter IV

Comprehensive discussion

4.1. Development of α-DC-ZZ-BNC

I hereby described the development of platform technology for next generation vaccine by utilizing ZZ-BNC, facilitating the *in vivo* pinpoint DDS in an antibody-dependent manner. In Chapter II, I have developed a DC-targeting ZZ-BNC by displaying α-CD11c IgGs on ZZ-BNC. The α-DC-ZZ-BNC could accumulate into DCs through either systemic (IV) or local (SC and IM) routes with comparable efficiency of other DC-targeting nanocarriers [1-3]. This efficient accumulation might be achieved by synergistic DC-targeting with α-CD11c IgGs and ZZ-BNC components (*i.e.*, ZZ domain, high mannose-type sugar chain, clustered Ags). Followed by the fusion with cationic LPs containing Ags, the α-DC-ZZ-BNC-LP-Ag complex could induce efficient Ag-specific IgG production through IV injection. However, the complex was less effective through SC injection, which might be caused by its positive charge. In Chapter III, for improving the particle properties, the α-DC-ZZ-BNC was conjugated with Ags by chemical crosslinking instead of LP fusion. Among vaccines examined, the α-DC-ZZ-BNC-Ag could induce more effective DC maturation without any adjuvant, followed by effective Ag-dependent CTL proliferation, Th-related immune responses, and Ag-specific IgGs production. Collectively, it was demonstrated that both DC-specific Ag-delivering ability and endogenous adjuvant activity of α-DC-ZZ-BNC contributed to the effective induction of cellular and humoral immunities.

4.2. DC-targeting molecules

The α-DC-ZZ-BNC complexes could accumulate to DCs efficiently (about 62% of splenic DCs through IV injection (see Fig. 2.4), about 10% of DCs in LNs through SC and IM injections (see Fig. 3.4, 3.5)). LPs displaying bacterial flagellin-related peptide could accumulate to about 20% of splenic DCs through IV injection [1]. The pH-responsive microparticles harboring α-CD205 IgGs could accumulate to about 30 % of DCs in ILN through SC injection [2]. The α-CD11c $F(ab)_2$-fused Ags could accumulate to about 81.4% of splenic DCs through SC injection [3]. These results indicated the α-DC-ZZ-BNC complexes harbors enough DC-targeting ability. For further improving the ability, since the ratio of α-CD11c IgG (mol) to ZZ-BNC (mol) was determined to be about 8 by based on previous studies [4], it is still necessary to optimize the ratio for maximizing the *in vivo* DC-targeting ability. Generally, as demonstrated with LPs displaying sugar chains [5], the targeting molecules displayed in a closed-packed manner do not always exhibit best targeting efficacy. Furthermore, while I chose α-CD11c IgG as a targeting molecule from IgGs against 5 DC-specific surface molecules (see Table 2.1), other IgGs recognizing the same surface molecules should be investigated for optimizing the DC targeting. Other DC-specific surface molecules (*e.g.*, CD205 [2, 6], Dectin-1 [6], FcR [7, 8]) are also promising, as they succeeded in inducing effective immunities by conjugating with Ags. From the viewpoint of cell biology on DCs, there are various subsets of DCs in body (see Fig. 4.1). Rigorous targeting of distinct DC subsets may be useful for regulating the balance between cellular and humoral immunity, encompassing the induction of most effective immune response against each pathogen. For instance, $CD8^+$ DCs possess highly-developed machinery for cross presentation of Ags, while low capability for cross presentation is observed in $CD8^-$ DCs [9]. If the

α-DC-ZZ-BNC complex can recognize with $CD8^+$ DCs rather than $CD8^-$ DCs, the complex can induce CTL-dependent cellular immunities preferentially (and *vice versa*).

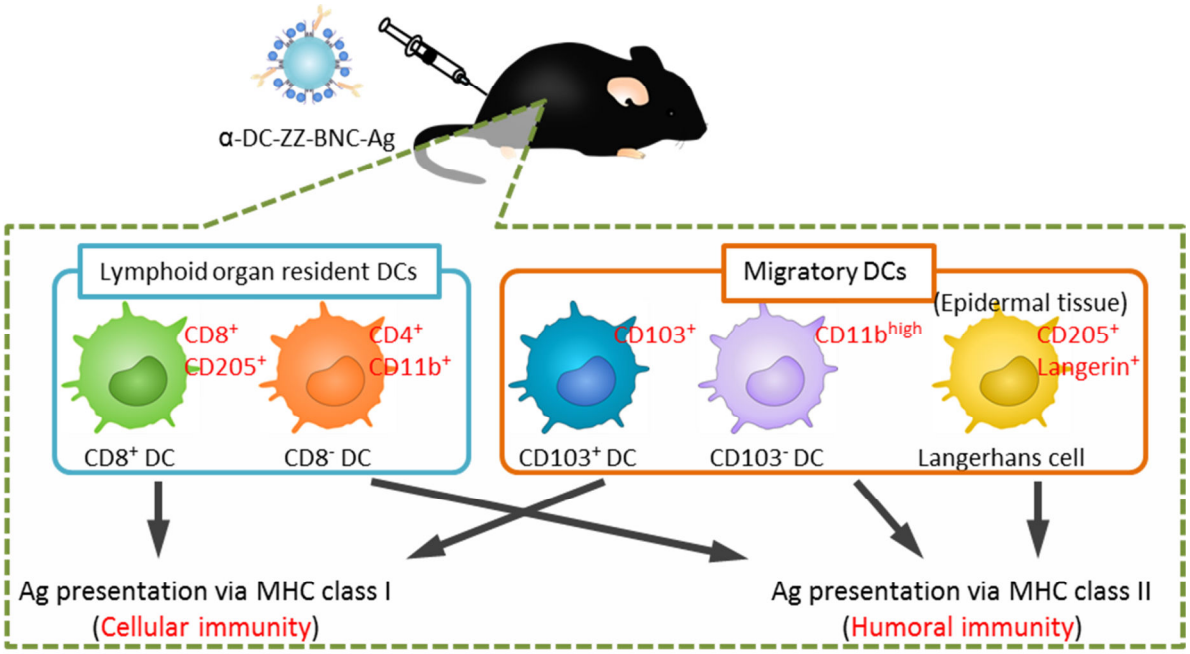

Fig. 4.1 Strategy for induction of effective immunities by targeting distinct DC subsets.
Red characters indicate highly-expressed molecules on respective DC subsets as targets.

Concerning about the DC-targeting ability of other molecules, ZZ-BNC components (*e.g.*, ZZ domains, high mannose-type sugar chains, clustered Ags) contributed to the *in vivo* accumulation to splenic DCs (Fig. 2.4). Although α-DC-ZZ-BNC showed highest accumulation efficiency (62% of $CD11c^+$ cells), ZZ-BNC and ZZ-domain-less BNC showed moderate and less efficiency (42% and 20% of $CD11c^+$ cells), respectively. Since ZZ-domain-less BNC possesses high mannose-type sugar chains and clustered Ags, it was indicated that ZZ domains by themselves harbor sufficient *in vivo* DC-targeting ability. If the ZZ domains of ZZ-BNC are replaced with other IgG Fc-binding domains of higher affinity (*e.g.*, B1 domain of *Streptococcal dysgalactiae* Protein G [10]), the modified ZZ-BNC would target DCs more efficiently. Additionally, the B1 domain of *Peptostreptococcus magnus* Protein L [11] could be used for displaying various types of Ig (including IgGs, IgMs, IgAs, IgEs, and IgDs) to expand the availability of α-DC Igs.

4.3. Adjuvant activity

Both α-DC-ZZ-BNC-Ag and ZZ-BNC-Ag could elicit effective *ex vivo* DC maturation without any adjuvant (Fig. 3.6). Because our facility was built under non-SPF conditions, it was very hard to examine if α-DC-ZZ-BNC-Ag could stimulate *in vivo* DC maturation more efficiently than ZZ-BNC-Ag or not. This situation has let us not to evaluate the contribution of α-CD11c IgG to *in vivo* DC maturation exactly. However, since other researchers reported that the Ag incorporation by α-CD11c IgG could induce effective DC maturation in a Toll-like receptor-independent manner [12], the α-CD11c IgG moiety of α-DC-ZZ-BNC-Ag may induce *in vivo* DC maturation. Next, it was clearly demonstrated that ZZ-BNC by itself harbors adjuvant activity and stimulates DC maturation at least *ex vivo*. It has not been determined what parts of

ZZ-BNC are recognized by DCs on the molecular basis, whereas two machineries could be involved in DC maturation. High mannose-type sugar chains displayed on ZZ-BNC may interact with CLRs (*e.g.*, DC-SIGN, DNGR-1) on DCs [13]. Clustered structure of ZZ-BNC may contribute to the prolonged release of antigens to maximize exposure to the immune system [14]. These interactions between ZZ-BNC and DCs could induce DC maturation and thereby elicit innate immunity.

4.4. Intracellular trafficking

Generally, vaccines are classified into two categories [15, 16]: prophylactic vaccines mainly elicit Ag-specific antibodies, contributing to the inhibition of pathogen invasion to host cells, pathogen opsonization, and complement fixation; and therapeutic vaccines mainly induce Ag-dependent CTL proliferation and Th1-related immunities, contributing to the elimination of infected and abnormal cells. Thus, the intracellular trafficking of Ags in DCs should be optimized to maximize the protective and/or therapeutic efficacy of DC-specific DDS-based vaccines. Cytoplasmic localization of delivered Ags is necessary for Ag presentation via MHC class I on DCs, leading to CTL proliferation (*i.e.*, cross presentation) [17, 18]. However, since the cross presentation occurs incidentally in DCs, conventional vaccines could not induce CTL-dependent cellular immunity efficiently. Accordingly, DC-targeting nanocarriers should deliver Ags into cytoplasm actively for exhibiting sufficient therapeutic effect of vaccines [19]. As described in Fig. 3.7B, both ZZ-BNC-OVA and α-DC-ZZ-BNC-OVA could enhance the OVA-specific CTL proliferation moderately and efficiently, respectively. It was speculated that the α-CD11c IgG could enhance the endosomal escape of OVA through the interaction with CR4 by help of HBV-derived membrane fusogenic activity of ZZ-BNC (see **3.5. Discussion**). But, it must be

analyzed whether the intracellular localization of delivered Ags in DCs is drastically changed from endosome to cytoplasm by the addition of α-CD11c IgG.

4.5. Liposomal fusion

After fusion with Ag-loaded cationic LPs, the α-DC-ZZ-BNC-LP-Ag complex could efficiently induce Ag-specific IgG production rather than Ag alone through IV injection. When administrated via SC route, non-specific bindings presumably caused by positive charge might reduce the recognition by DCs in LNs, and then elicited less Ag-specific immunity (see Table 3.1 and Fig. 3.1). As described in Chapter III, to improve the particle properties, the α-DC-ZZ-BNC was conjugated chemically with Ags. The complex expectedly exhibited excellent Ag-specific immune responses through SC injection. However, it is premature to get rid of the use of LPs for DC-specific BNC-based vaccines. Previous studies indicated that BNC can form stable complex not only with cationic LPs but also with anionic LPs [20]. When substantial amount of Ags are successfully encapsulated into anionic or neutral LPs, the α-DC-ZZ-BNC could be fused with the LPs and then used for DC-specific BNC-based vaccines. The incorporation of phospholipids that destabilize endosomal membrane by the formation of inverted hexagonal II phase under acidic conditions (*e.g.*, dioleyl phosphatidylethanolamine (DOPE)) into LPs would be useful for enhancing endosomal escape of Ags. The modification of LPs with pH-responsive polymer that shows membrane fusion with endosomal membrane under acidic condition [21] could also be applicable for the same purpose. These approaches are considered promising for induction of potent CTL-dependent cellular immunity.

It has been well known that conventional LP-based medicines administrated IV are promptly trapped by reticuloendothelial system (RES) in liver, lung, spleen, and so

on [22]. Recently, our group found that LPs modified with BNCs can evade from the RES entrapment *in vivo*, since BNCs significantly reduce the opsonization of LPs by recruiting serum albumin (Takagi *et al*., submitted). Thus, the α-DC-ZZ-BNC-based vaccines (including α-DC-ZZ-BNC-Ag and α-DC-ZZ-BNC-LP-Ag) would be more stable than conventional nanomedicines *in vivo*. When administration route is changed from IV to SC or IM, the α-DC-ZZ-BNC-based vaccines could become more effective.

4.6. Issues to be addressed before clinical applications

In this thesis, I have successfully developed a platform technology for DC-specific BNC-based vaccines. However, the vaccines described herein are available only in mice, because DC-targeting IgG is specific to mouse CD11c molecule. While ZZ-BNC is expected to be recognized by DCs from many animals, α-DC-ZZ-BNC is considered not operative in other animals. For expanding the possibility of α-DC-ZZ-BNC, it is prerequisite to replace α-mouse CD11c IgG with α-human CD11c IgG. Furthermore, the molecular mass of α-DC-ZZ-BNC-OVA vaccine is estimated approximately 12.6 MDa, composed of 6-MDa ZZ-BNC, 1.2-MDa α-CD11c IgG (8 molecules), and 5.4-MDa OVA (120 molecules). For maximizing the vaccine efficacy and minimizing the IgG-derived side effects, the ratio of α-CD11c IgG should be reduced by utilizing small α-CD11c molecules (*e.g.*, single chain Fv against α-human CD11c).

Recently, cancer immunotherapy has been performed by using DC-targeting vaccines for eliciting CTL proliferation and Th1-dependent immunity in a cancer-specific Ag-dependent manner [23]. In this thesis, it was demonstrated that α-DC-ZZ-BNC-Ag vaccines could induce Ag-specific cellular immunity effectively.

Therefore, α-DC-ZZ-BNC could be used for the forthcoming cancer vaccines by incorporating cancer-specific Ags.

4.7. References

1. A. Faham, J.G. Altin, Antigen-containing liposomes engrafted with flagellin-related peptides are effective vaccines that can induce potent antitumor immunity and immunotherapeutic effect, J. Immunol. 185 (2010) 1744–1754.
2. Y.J. Kwon, E. James, N. Shastri, J.M.J. Fréchet, *In vivo* targeting of dendritic cells for activation of cellular immunity using vaccine carriers based on pH-responsive microparticles, Proc. Natl. Acad. Sci. U. S. A. 102 (2005) 18264–18268.
3. H. Wei, S. Wang, D. Zhang, S. Hou, W. Qian, B. Li, H. Guo, G. Kou, J. He, H. Wang, Y. Guo, Targeted delivery of tumor antigens to activated dendritic cells via CD11c molecules induces potent antitumor immunity in mice, Clin. Cancer Res. 15 (2009) 4612–4621.
4. M. Iijima, T. Matsuzaki, N. Yoshimoto, T. Niimi, K. Tanizawa, S. Kuroda, Fluorophore-labeled nanocapsules displaying IgG Fc-binding domains for the simultaneous detection of multiple antigens, Biomaterials. 32 (2011) 9011–9020.
5. M. Hirai, H. Minematsu, N. Kondo, K. Oie, K. Igarashi, N. Yamazaki, Accumulation of liposome with Sialyl Lewis X to inflammation and tumor region: application to *in vivo* bio-imaging, Biochem. Biophys. Res. Commun. 353 (2007) 553–558.
6. R.W. Carter, C. Thompson, D.M. Reid, S.Y.C. Wong, D.F. Tough, Preferential induction of $CD4^+$ T cell responses through *in vivo* targeting of antigen to dendritic cell-associated C-type lectin-1, J. Immunol. 177 (2006) 2276–2284.

7. K. Serre, P. Machy, J.C. Grivel, G. Jolly, N. Brun, J. Barbet, L. Leserman, Efficient presentation of multivalent antigens targeted to various cell surface molecules of dendritic cells and surface Ig of antigen-specific B cells, J. Immunol. 161 (1998) 6059‑6067.

8. K. Serre, L. Giraudo, L. Leserman, P. Machy, Liposomes targeted to Fc receptors for antigen presentation by dendritic cells *in vitro* and *in vivo*, Methods Enzymol. 373 (2003) 100–118.

9. O.P. Joffre, E. Segura, A. Savina, S. Amigorena, Cross-presentation by dendritic cells., Nat. Rev. Immunol. 12 (2012) 557–569.

10. U. Sjöbring, L. Björck, W. Kastern, Streptococcal protein G. Gene structure and protein binding properties, J. Biol. Chem. 266 (1991) 399-405.

11. W. Kaster, U. Sjöbring, L. Björck, Structure of peptostreptococcal protein L and identification of a repeated immunoglobulin light chain-binding domain, J. Biol. Chem. 267 (1992) 12820-12825.

12. A.L. White, A.L. Tutt, S. James, K.A. Wilkinson, F.V. Castro, S.V. Dixon, J. Hitchcock, M. Khan, A. Al-Shamkhani, A.F. Cunningham, M.J. Glennie, Ligation of CD11c during vaccination promotes germinal centre induction and robust humoral responses without adjuvant, Immunology 131 (2010) 141–151.

13. M.J. Robinson, D. Sancho, E.C. Slack, S. LeibundGut-Landmann, C. Reis e Sousa, Myeloid C-type lectins in innate immunity, Nat. Immunol. 7 (2006) 1258–1265.

14. A.E. Gregory, R. Titball, D. Williamson, Vaccine delivery using nanoparticles, Front. Cell. Infect. Microbiol. 3 (2013) 1-13.

15. M.F. Bachmann, G.T. Jennings, Vaccine delivery: a matter of size, geometry, kinetics and molecular patterns, Nat. Rev. Immunol. 10 (2010) 787–796.

16. J.W. Yewdell, Designing $CD8^+$ T cell vaccines: it's not rocket science (yet)., Curr. Opin. Immunol. 22 (2010) 402–410.

17. E.S. Trombetta, I. Mellman, Cell biology of antigen processing *in vitro* and *in vivo*, Annu. Rev. Immunol. 23 (2005) 975–1028.

18. J. Banchereau, F. Briere, C. Caux, J. Davoust, S. Lebecque, Y. Liu, B. Pulendran, K. Palucka, Immunobiogy of dendritic cells, Immunology 18 (2000) 767–811.

19. P.J. Tacken, I.J.M. de Vries, R. Torensma, C.G. Figdor, Dendritic-cell immunotherapy: from *ex vivo* loading to *in vivo* targeting, Nat. Rev. Immunol. 7 (2007) 790–802.

20. J. Jung, T. Matsuzaki, K. Tatematsu, T. Okajima, K. Tanizawa, S. Kuroda, Bio-nanocapsule conjugated with liposomes for *in vivo* pinpoint delivery of various materials., J. Control. Release 126 (2008) 255–264.

21. E. Yuba, Y. Kono, A. Harada, S. Yokoyama, M. Arai, K. Kubo, K. Kono, The application of pH-sensitive polymer-lipids to antigen delivery for cancer immunotherapy, Biomaterials 34 (2013) 5711–5721.

22. S. Stolnik, L. Illum, S.S. Davis, Long circulating microparticulate drug carriers, Adv. Drug Deliv. Rev. 16 (1995) 195–214.

23. K. Palucka, J. Banchereau, Cancer immunotherapy via dendritic cells, Nat. Rev. Cancer. 12 (2012) 265–277.

Acknowledgements

This is a thesis to be submitted to the Graduate School of Bioagricultural Sciences, Nagoya University for the Ph.D. of agriculture. The works described in this thesis have been performed from 2011 to 2014 under supervision of Prof. Shun'ichi Kuroda at the Laboratory of Industrial Bioscience, Division of Biotechnology, Department of Bioengineering Sciences, Graduate School of Bioagricultural Science, Nagoya University.

First of all, my deepest and sincere gratitude goes to Prof. Shun'ichi Kuroda whose comments and suggestions were innumerably valuable throughout the course of my study. I am grateful to Prof. Shinji Nagata and Prof. Hisashi Muramatsu at the Kochi University, Prof. Katsuyuki Tanizawa for their valuable advices and warm encouragements. I would like to acknowledge Prof. Hideo Nakano, Prof. Tsukasa Matsuda, Prof. Andrés D. Maturana, and Prof. Hideki Shibata whose comments made enormous contributions toward my work, Prof. Masumi Iijima and Prof. Nobuo Yoshimoto for their technical supports and warm encouragements, Prof. Takeshi Arakawa at University of the Ryukyus, Prof. Yasunobu Matsumoto at the University of Tokyo, Dr. Tomomitsu Sewaki, Dr. Senji Tafuku, Dr. Takeshi Miyata, and Dr. Tetsuya Harakuni for providing antigens and performing infection experiments. I sincerely express my thanks to all member of Prof. Kuroda's laboratory.

Finally, I would also like to express my gratitude to my family for their mental and financial supports, and warm encouragements.

List of publications (related to this thesis)

Original papers

1. **H. Matsuo**, N. Yoshimoto, M. Iijima, T. Niimi, J. Jung, S.Y. Jeong, E.K. Choi, T. Sewaki, T. Arakawa, S. Kuroda, Engineered hepatitis B virus surface antigen L protein particles for *in vivo* active targeting of splenic dendritic cells, Int. J. Nanomedicine 7 (2012) 3341-3350. (H.M. performed all experiments and prepared the entire manuscript.)

2. **H. Matsuo**, S. Tafuku, M. Tomioka, S. Yokoi, M. Iijima, N. Yoshimoto, T. Niimi, A.D. Maturana, T. Sewaki, T. Arakawa, S. Kuroda, Bio-nanocapsules harboring viral infection and dendritic cell-targeting machineries for *in vivo* immunization, J Control. Release (2013) in preparation. (H.M. performed all experiments and prepared the entire manuscript.)

Reference paper

1. T. Miyata, S. Tafuku, T. Harakuni, M. Tadano, N. Yoshimoto, M. Iijima, **H. Matsuo**, G. Matsuzaki, S. Kuroda,T. Arakawa, A bio-nanocapsule containing envelope protein domain III of Japanese encephalitis virus protects mice against lethal Japanese encephalitis virus infection, Microbiol. Immunol. 57 (2013) 470-477. (H.M. performed a part of experiments.)

Presentations at international conferences (*Speaker)

1. ***H. Matsuo**, K. Miyabe, N. Yoshimoto, M. Iijima, S. Kuroda, *In vivo* active delivery of antigens to splenic dendritic cells by engineered bio-nanocapsules, hepatitis B virus surface antigen L protein particle (Poster), Engineering Conference International Vaccine Technology IV, Albufeira, Portugal (2012)

2. ***H. Matsuo**, M. Tomioka, N. Yoshimoto, M. Iijima, S. Kuroda, *In vivo* active delivery of antigens with dendritic cell-targeting bio-nanocapsules (Oral), Vaccine Delivery and Stabilization: Improving the Reach of Vaccines, Boston, USA (2013)

Presentation at domestic meetings (*Speaker)

1. ***松尾英典**、 良元伸男、黒田俊一, 樹状細胞標的化バイオナノカプセルの開発 (Oral), 第 34 回 日本分子生物学会年会 (2011)

2. ***松尾英典**、宮部 康平、飯嶋 益巳、良元 伸男、黒田 俊一, ワクチン抗原の能動的送達を可能にする樹状細胞標的化バイオナノカプセルの開発 (Oral), 第 28 回 日本 DDS 学会年会 (2012)

3. *富岡三貴、**松尾英典**、黒田俊一, 樹状細胞標的化バイオナノカプセルを用いた DNA ワクチンの開発 (Oral), 第 35 回 日本分子生物学会年会 (2012)

4. *富岡三貴、**松尾英典**、黒田俊一, 樹状細胞標的化バイオナノカプセルを用いた高免疫原性 DNA ワクチンの開発 (Oral), 第 29 回 日本 DDS 学会年会 (2013)

Review

1. 松尾英典、良元伸男、黒田俊一, バイオナノカプセルを用いた生体内ピンポイント DDS 技術の開発, 月刊表面 50 (2013) 207-218.

Patent

1. 黒田俊一、松尾英典、良元伸男、飯嶋益巳、新川武, バイオナノカプセル及びリポソームを含む複合体

   特願２０１２－０８０７９１（平成２４年３月３０日）

   PCT/JP2013/059691 （平成２５年３月２９日）

   日本国特許成立（平成２５年１１月２６日）

Award

1. **H. Matsuo**, Development of highly immunogenic vaccine by using dendritic cell-targeting bio-nanocapsule, Poster Award in IGER Annual meeting 2013.

List of other publication

Original paper

1. H. Muramatsu, **H. Matsuo,** N. Okada, M. Ueda, H. Yamamoto, S. Kato, S. Nagata, Characterization of ergothionase from *Burkholderia* sp. HME13 and its application to enzymatic quantification of ergothioneine, Appl. Microbiol. Biotechnol. 12 (2013) 5389-5400. (H.M. performed a part of experiments.)

*Presentation at domestic meetings (*Speaker)*

1. *松尾英典、柳舘勇、山本由徳、吉田徹志、Y. B. Pasolon、F. S. Rembon、E.Tenda、R. B. M. kay、宮崎彰, インドネシア・南東スラウェシ州ムナ島および北スラウェシ州サンギヘ島におけるアレンガ属ヤシの生育特性とデンプン生産性 (Oral), 日本作物学会四国支部第 45 回講演会(2008)

2. *柳舘勇、山本由徳、吉田徹志、Y. B. Pasolon、F. S. Rembon、E.Tenda、R. B. M. kay、松尾英典、宮崎彰, アレンガ属ヤシの栽培と利用 ： インドネシア国南東スラウェシ州ムナ島および北スラウェシ州サンギヘ島における事例 (Oral), 日本作物学会四国支部第 45 回講演会(2008)

3. *松尾英典、村松久司、上田桃子、山本浩明、加藤伸一郎、永田信治, *Burkholderia* sp. HME13 由来エルゴチオナーゼの精製と諸性質 (Oral), 日本農芸化学 2011 年度大会 (2011)

4. *尾崎旬、竹山純、松尾英典、上田桃子、山本浩明、加藤伸一郎、村松久司、永田信治, D-フェニルセリンデアミナーゼを用いた L-threo-フェニルセリン生産法 (Oral), 第 53 回日本生化学会中国・四国支部例会 (2012)

5. *栗田周哉、宮奥晴菜、**松尾英典**、松井祐士，加藤伸一郎、村松久司、永田信治, *Burkholderia* sp. HME13 由来新奇チオールウロカニン酸代謝酵素遺伝子の同定 (Oral), 日本農芸化学会中四国支部第３５回講演会 (2013)

6. *村松久司，宮奥晴菜，栗田周哉，**松尾英典**，加藤伸一郎，永田信治，*Burkholderia* sp. HME13 由来チオールウロカニン酸代謝酵素の遺伝子クローニングと精製 (Poster), 第 86 回日本生化学会大会 (2013)